Hollow Titanium Dioxide Nanoparticles as Sunscreen Agent in Sunscreen

Nichapat Pukveera

A Report Submitted in Partial Fulfillment of the Requirements
for the Degree of Bachelor of Engineering (Petrochemical Engineering)
Department of Chemical Engineering, School of Engineering,
King Mongkut's Institute of Technology Ladkrabang
Academic Year 2020

อนุภาคกลวงของนาโนไทเทเนียมไดออกไซด์เพื่อเป็นสารป้องกันแสงแดด ในครีมกันแดด

ณิชาภัทร พุกวีระ

ปริญญานิพนธ์นี้เป็นส่วนหนึ่งของการศึกษาตามหลักสูตร

วิศวกรรมศาสตรบัณฑิต สาขาวิชาวิศวกรรมปิโตรเคมี

ภาควิชาวิศวกรรมเคมี คณะวิศวกรรมศาสตร์

สถาบันเทคโนโลยีพระจอมเกล้าเจ้าคุณทหารลาดกระบัง

ปีการศึกษา 2563

Title	Hollow Titanium Dioxide Nanoparticles as Sunscreen Agent in Sunscreen
By	Ms. Nichapat Pukveera
Field of Study	Petrochemical Engineering
Advisor	Asst. Prof. Dr. Teeraporn Suteewong Department of Chemical Engineering, School of Engineering, King Mongkut's Institute of Technology Ladkrabang

Accepted by the School of Engineering, King Mongkut's Institute of Technology Ladkrabang in Partial Fulfillment of the Requirements for the Degree of Bachelor of Engineering (Petrochemical Engineering).

Thesis Committee

TEERAPORN
_____ Chairman
(Asst. Prof. Dr. Teeraporn Suteewong)

Duangkamol
_____ Committee
(Assoc. Prof. Dr. Duangkamol Na-Ranong)

Kriangsak
_____ Committee
(Assoc. Prof. Dr. Kriangsak Kraiwattanawong)

Title	Hollow Titanium Dioxide Nanoparticles as Sunscreen Agent in Sunscreen
By	Ms. Nichapat Pukveera
Advisor	Asst. Prof. Dr. Teeraporn Suteewong
Field of Study	Petrochemical Engineering
Year	2020
Affiliation	Department of Chemical Engineering, School of Engineering, King Mongkut's Institute of Technology Ladkrabang

Abstract

Nowadays, there is the environmental concern especially marine ecosystems and coral bleaching caused by the accumulation of TiO_2 NPs from sunscreen. Due to its photocatalytic properties, TiO_2 NPs can generate reactive oxygen species (ROS) that are high harmful to biomolecules. Thus, increasing their UV shielding performance could lower the amount of TiO_2 NPs used in sunscreen. It could be done by modifying light scattering efficiency of TiO_2 NPs. In this study, instead of widely used dense TiO_2 NPs, hollow TiO_2 NPs (h-TiO_2 NPs) were prepared due to their large surface area, low density, and high light scattering. Silica core nanoparticles (SiO_2) with average particle sizes of 30 to 270 nm, were first synthesized via the Stöber method, by controlling the silica precursor (tetraethyl orthosilicate; TEOS) and catalyst (ammonium hydroxide; NH_4OH) concentrations. Then, various concentration of titanium tetrabutoxide (TBT) was added in the SiO_2 core suspension to grow the TiO_2 shell on surface via two different sol-gel methods i.e., modified sol-gel (I) and simple yet robust process (II). The presence of NH_4OH catalyst, promote the condensation and formation of thicker shell. Particle with thinner shell thickness has better light absorbance but lower light scattering. In this study, based on particle size and absorbing volume, h-TiO_2-3.25 and h-TiO_2-6.49 NPs prepared by method I were suitable for used as sunscreen agent.

Keywords: TiO_2, Hollow nanoparticles, Sunscreen agent, Coating

เรื่อง	อนุภาคกลวงของนาโนไทเทเนียมไดออกไซด์เพื่อเป็นสารป้องกันแสงแดด ในครีมกันแดด
โดย	นางสาวณิชาภัทร พุกวีระ
อาจารย์ที่ปรึกษา	ผศ. ดร. ธีรพร สุธีวงศ์
สาขาวิชา	วิศวกรรมปิโตรเคมี
ปีการศึกษา	2563
สังกัด	ภาควิชาวิศวกรรมศาสตร์ คณะวิศวกรรมศาสตร์ สถาบันเทคโนโลยีพระจอมเกล้าเจ้าคุณทหารลาดกระบัง

บทคัดย่อ

ในปัจจุบันมีความกังวลด้านสิ่งแวดล้อมโดยเฉพาะระบบนิเวศทางทะเลและการฟอกขาวของปะการังที่เกิดจากการสะสมของอนุภาคนาโนของไทเทเนียมไดออกไซด์ที่เป็นส่วนประกอบสำคัญในครีมกันแดด โดยอนุภาคนาโนของไทเทเนียมไดออกไซด์มีสมบัติการเร่งปฏิกิริยาด้วยแสงที่ดี ก่อให้เกิดอนุมูลอิสระของอนุพันธ์ออกซิเจนอิสระที่ว่องไวซึ่งเป็นอันตรายต่อสารชีวโมเลกุลได้อย่างรวดเร็ว ดังนั้นการเพิ่มประสิทธิภาพของอนุภาคนาโนไทเทเนียมไดออกไซด์ในการป้องกันรังสีอัลตร้าไวโอเลตอาจช่วยลดปริมาณอนุภาคนาโนไทเทเนียมไดออกไซด์ที่ใช้ในครีมกันแดด ซึ่งสามารถทำได้โดยการเพิ่มความสามารถการกระเจิงแสง ในงานวิจัยนี้จึงพัฒนาแบบกลวงขึ้นมาเพื่อแทนการใช้อนุภาคนาโนของไทเทเนียมไดออกไซด์แบบตันที่ใช้กันอย่างแพร่หลาย เนื่องจากมีพื้นที่ผิวมาก ความหนาแน่นต่ำและการกระเจิงของแสงสูง โดยทำการสังเคราะห์อนุภาคนาโนซิลิกาที่มีขนาด 30 ถึง 270 นาโนเมตรด้วยวิธีสโตเบอร์ (Stöber method) เพื่อใช้เป็นอนุภาคแกน โดยการควบคุมความเข้มข้นของเตตระเอธิลออร์โธซิลิเกต (TEOS) เป็นสารตั้งต้นซิลิกาและแอมโมเนียมไฮดรอกไซด์ (NH_4OH) เป็นตัวเร่งปฏิกิริยา จากนั้นทำการสังเคราะห์อนุภาคนาโนไทเทเนียมไดออกไซด์กลวง (h-TiO_2 NPs) โดยใช้ไทเทเนียมเตตระบิวทอกไซด์ (TBT) เป็นสารตั้งต้นเกิดปฏิกิริยาผ่านกระบวนการโซล-เจลบนผิวซิลิกา โดยศึกษาวิธีการหุ้ม 2 วิธีคือ modified sol-gel (I) และ simple yet robust process (II) จากการศึกษาพบว่าการระบบที่มีตัวเร่งปฏิกิริยาส่งผลให้ชั้นเปลือกของไทเทเนียมไดออกไซด์มีความหนามากกว่าเนื่องจากตัวเร่งปฏิกิริยาส่งผลให้อัตราการควบแน่นสูงขึ้น อนุภาคที่มีชั้นเปลือกบางมีค่าการดูดซับแสงสูงแต่มีการกระเจิงแสงต่ำ ในการศึกษานี้พบว่าเมื่อพิจารณาที่ขนาดและปริมาตรการดูดซับแสง อนุภาค h-TiO_2-3.25 และ h-TiO_2-6.49 ที่สังเคราะห์จากวิธีที่ I เหมาะสมสำหรับการใช้เป็นสารป้องกันแสงแดด

คำสำคัญ: TiO_2 อนุภาคกลวง สารป้องกันแสงแดด การเคลือบ

Acknowledgements

First, I would like to express my appreciation to National Science and Technology Development Agency (NSTDA) for funding support under the contract for a research scholarship to prepare a thesis for the Young Scientist and Technologist Program (YSTP) No. SCA-CO-2563-12312-TH.

I would like to express my sincere gratitude to Dr. Duangporn Polpanich, researcher of National Nanotechnology Center (NANOTEC) for giving me an opportunity and providing invaluable guidance during this thesis.

I would also like to extend my gratitude Asst. Prof. Dr. Teeraporn Suteewong, my advisor, who suggest me the golden opportunity to do this thesis under the YSTP, for her guidance and providing me with all facility that was required in this thesis.

Next, I sincerely thank to Assoc. Prof. Dr. Duangkamol Na-Ranong and Assoc. Prof. Dr. Kriangsak Kraiwattanawong, thesis committee, and every professor in department for their recommendation and opinion.

Finally, I am extremely grateful to my parents and friends for their support, helping and encouraging me throughout the year.

Nichapat Pukveera

Table of Contents

List of Figures

List of Tables

Page

CHAPTER I

INTRODUCTION

1.1 Background

Sunlight is one of the most important energies of the world and life. It helps us see things, keeps the body warm and contributes to the photosynthesis. In addition, at present, sunlight is used to generate electricity. But, if being excessively exposed to sunlight, human can encounter negative effects such as sunburn, premature aging, heat stroke and skin cancer[1]. Due to the destruction of the current ozone layer, the intensity of ultraviolet (UV) radiation that reaches the Earth has been increasing. As a result, the risk of solar hazards increases.

UV ray part of the spectrum of electromagnetic radiation can be classified by wavelength into three types: UVA (315-400 nm), UVB (280-315 nm) and UVC (100-280 nm) rays[2]. 90-95% of UVB is absorbed by the ozone layer. UVB rays can pass through the outer layer of the skin (the epidermis) and is the main cause of skin burning. 95% of UVA can reach the Earth's surface, which can pass through the middle layer of the skin (the dermis)[3] and is also the main cause of skin aging. UVA and UVB rays can damage DNA in cells, which causes skin cancer. Therefore, sun protection is important and can be done in several ways, such as wearing long sleeves and long pants, using an umbrella when going outdoors, wearing a wide-brimmed hat and sunglasses, and using a sunscreen with an appropriate amount and regularly. The use of sunscreens is one of the most popular ways to protect the skin from UV damage. First appeared in commerce of sunscreen in USA in the 1920s[4]. Sunscreen can be classified according to the mechanism of sun protection into two types: physical and chemical sunscreens. Chemical sunscreens contain absorbent chemicals such as oxybenzone, octinoxate, octisalate and avobenzone etc. UV rays are converted into heat energy, which is later released from the skin. In part of physical sunscreen, it contains particles that can reflect and scatter UV rays. The most popular particles are dense or non-hollow titanium dioxide (TiO_2) and zinc oxide (ZnO) particles. These are both UVA and UVB resistant. TiO_2 is one of the most popular sunscreen agents used in inorganic sunscreens with ZnO because of chemically stable and undergo negligible dissolution under normal environmental conditions[5]. To increase the protection efficiency, large amount of TiO_2 nanoparticles is required. This, however, stimulate the environment concern especially marine ecosystems and coral bleaching caused by TiO_2 and ZnO NPs in sunscreen. In the Goldschmidt geochemistry conference, Dr. Labille[6] (2018) reported that TiO_2 nanoparticles tend to lose their protective coating under the influence of UV light or seawater, resulting in TiO_2 has more toxic to the aquatic environment. In the two months of high summer, titanium dioxide was released around 54 kg which is a significant amount. They anticipate an accumulation of titanium dioxide in the seashore littoral, which can affect wildlife. If titanium dioxide is used in areas where stagnant water, such as swimming pools, it will increase an accumulation of titanium dioxide. Because of concentrated TiO_2 in the aquatic environment can be harmful to fish and other organisms, the quantities of TiO_2 should be reduced. To lower the amount of TiO_2 in physical sunscreen, modification of TiO_2 NPs in term of light scattering efficiency should be modified.

There are many studied that support the advantage properties of hollow structure. Chen et al.[7] (2005) synthesized the hollow gold nanocage that strongly absorb light in the near-IR region higher than organic dye. Thus, it is suitable for used as an optical coherence tomography contrast agent. Hollow particles have interesting optical properties. Because of the cavity within the particle can cause internal multiple light scattering and reflections[8]. Wang et al.[9] (2017) synthesized bio-inspired dopamine-melanin solid nanoparticles (Dpa-s NPs) and hollow nanoparticles (Dpa-h NPs) as UV-absorbers in polymer. They reported that compared with Dpa-s NPs, Dpa-h NPs allows multiple reflections of UV light within the interior cavity, leading to more efficient absorption of UV light and therefore offering an improved UV-shielding activity.

In this research, we aim to synthesize the hollow TiO_2 NPs (h-TiO_2 NPs) to increase scatter efficiency in sunscreen. The silica core nanoparticles (SiO_2 NPs) were synthesized by the Stöber method using tetraethyl orthosilicate (TEOS) as the precursor and ammonium hydroxide (NH_4OH) as the catalyst. h-TiO_2 NPs are synthesized by two different sol-gel methods using titanium tetrabutoxide (TBT) as the titania precursor. SiO_2 core were removed by selective etching. As control, dense TiO_2 NPs were synthesized using titanium tetraisopropoxide (TTIP) as a precursor. Effect of the morphology, shell thickness and particle size of h-TiO_2 NPs will be studied. Thus, if we compare the hollow and dense spherical TiO_2 particles, the hollow spherical TiO_2 particles allow light to be more scattered and reflected better than dense spherical TiO_2 particles[8]. For this reason, hollow spherical TiO_2 particles are attractive to be used as sunscreen agents.

1.2 Objectives

1.2.1 To synthesize h-TiO_2 NPs with different shell thickness.

1.2.2 To study the effects of size and morphology of h-TiO_2 NPs on optical properties.

1.3 Scopes of Work

1.3.1 Synthesis of spherical h-TiO_2 NPs with different particle sizes and shell thickness

1.3.2 Characterization of spherical h-TiO_2 NPs

1.4 Expected Output

1.4.1 h-TiO_2 NPs with improved sun protection efficiency.

CHAPTER II

LITERATURE REVIEW

2.1 Sunscreen

2.1.1 Chemical sunscreen

Chemical sunscreens (or known as organic sunscreen) contain an organic compound as active ingredient that have absorbent properties. UV rays are converted into heat energy and then heat is released from the skin. Mechanism of chemical sunscreen are showed in Fig. 2-1. Chemical sunscreen agents are not durable, cause more irritation than physical sunscreen. Chemical ingredients can cause skin reactions, including acne, burning, dryness, blisters, itching, redness, rash, swelling, stinging, and tightening of the skin[10].

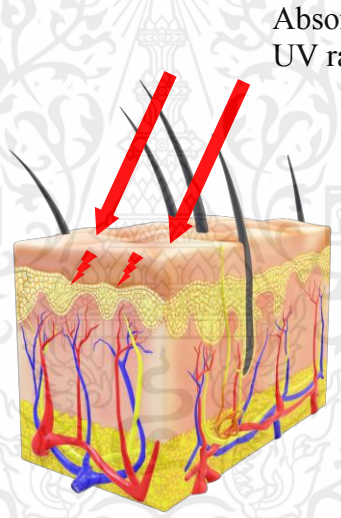

Figure 2-1 Mechanism of chemical sunscreen.

The organic absorbers are commonly aromatic compounds conjugated with a carbonyl group that can classified by chemical structure into seven groups: (1) Cinnamate derivatives, (2) para-Aminobenzoate derivatives, (3) Salicylate derivatives, (4) Camphor derivatives, (5) Benzophenone derivatives, (6) Anthranilate derivatives and (7) Dibenzoyl methane derivatives as showed in Fig. 2-2.

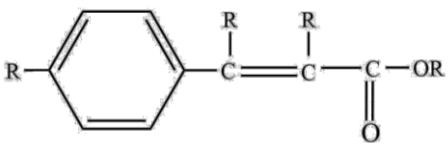

Cinnamate derivatives

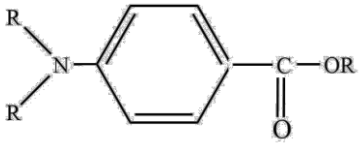

para-Aminobenzoate derivatives

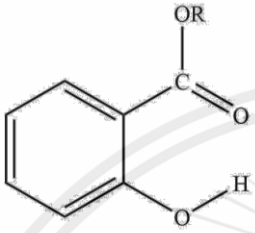

Salicylate derivatives

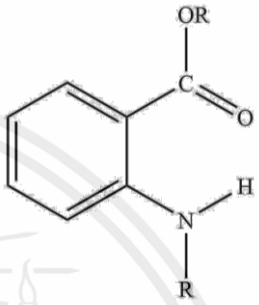

Anthranilate derivatives

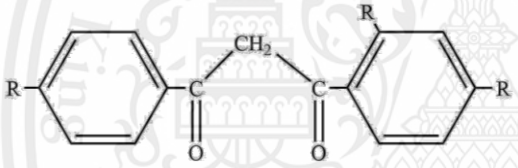

Dibenzoyl methane derivatives

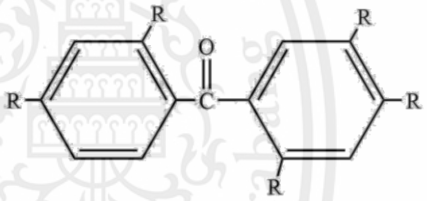

Benzophenone derivatives

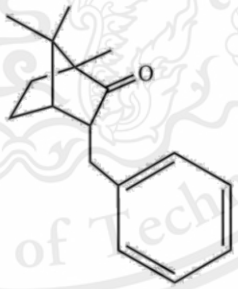

Camphor derivatives

Figure 2-2 Seven groups of organic chemical sunscreen filters.
Adapted from International Agency for Research on Cancer. Chemical and Physical Characteristics of Sunscreen Constituents. In *IARC Handbooks of Cancer Prevention Volume 5*; 2001; pp 17–21.

Benzophenone derivatives, anthranilate and dibenzoyl methane are UVA absorbers, while cinnamates, para-Aminobenzoate derivatives, salicylate and camphor derivatives are UVB absorbers[4]. Organic sunscreens are often used in combination because they do not have a single organic sunscreen, which is used at a level approved by the US Food and Drug Administration[11].

para-Aminobenzoate (PABA) was popular organic sunscreen in the 1950s and 1960s. Reaction of para-aminobenzoic acid (PABA)-based sunscreens can cause some symptoms such as acne, burning, itching, and redness. Ethylhexyl dimethyl PABA can induce in phototoxicity and photomutagenicity in budding yeast cells.

Cinnamate have improved over the years. Ethylhexyl methoxycinnamate is derivative of cinnamate that is the most popular chemical sunscreen because its good UVR absorption, oil solubility, water insolubility. So, it is use in waterproof sunscreen formulations.

Salicylate was the first UVR filters, can be easily incorporated into cosmetic formulations, some are used to solubilize other insoluble cosmetic ingredients, such as benzophenones. Homosalate and ethylhexyl salicylate are derivatives of salicylate the are the most used in sunscreen preparations.

Camphor derivatives are bicyclic compounds which are solid. Camphor derivatives are approved for use in Europe but not in the USA.

Dibenzoylmethanes are one of UVA filters, it has a low photostability. Butyl methoxydibenzoylmethane is derivative of dibenzoylmethanes that was introduced in 1978 in Europe as a sunscreen ingredient. The first formulation containing butyl methoxydibenzoylmethane is reported that loss of efficiency during use because of photoreaction occurs.

Benzophenones are dibenzoylmethane derivatives that are concern about safety because its aromatic ketones are more difficult to detoxify than esters and its solid state resulting in loss of solubility in cosmetic formulations. When high SPFs is needed, benzophenone-3 is usually used in combinations with solubilizers.

Anthranilates such as menthyl anthranilate, are stable and safe and have no significant solvent effects in cosmetic formulations like salicylates.

Because of absorption of UV radiation rather than reflect or scatter of organic sunscreen that make it vulnerable photo-degradation and tend to occur free radicals. However, the main concern with organic sunscreens is the chance of photo-irritant or photo-sensitizing reactions in sensitive skin[12].

2.1.2 Physical sunscreen

Physical or inorganic sunscreen contains an inorganic compound as active ingredient. It physically reflects or scatters the UV radiation[13], unlike organic active ingredient which can only absorb. Mechanism of chemical sunscreen are showed in Fig. 2-3. Some of inorganic materials such as iron oxide and cerium oxide can be used as

sunscreen agents, but it has poor UV protection[14]. The most popular inorganic absorbers are titanium dioxide (TiO_2) and zinc oxide (ZnO) nanoparticles. These are both UVA and UVB resistant, and less irritation than chemical sunscreen because they do not typically cause allergic reactions. But it causes a thick, sticky texture in sunscreen. Inorganic absorbers are commonly used in combination with organic absorbers to achieve high sun protection factor (SPF) value. The effectiveness of sunscreen is qualified by sun protection factor (SPF) that is the UV energy required producing a minimal erythema dose (MED) on protected skin, divided by the UV energy required to produce a MED on unprotected skin[15]. SPF is a measure of protection against UVB radiation, it has no bearing on UVA rays[16].

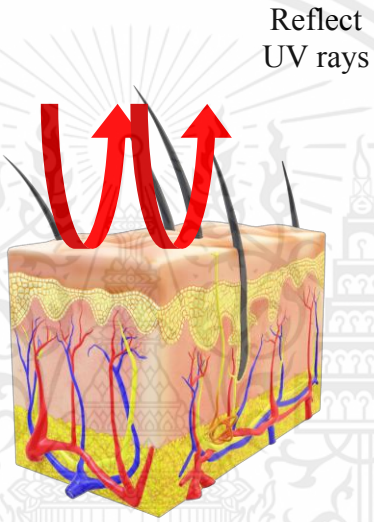

Figure 2-3 Mechanism of physical sunscreen.

TiO_2 and ZnO particles are generally used at a size of 200–300 nm, which results in low UV protection efficiency because 200 nm particles are scatter strongly at wavelengths more than UV region. These size regime makes them opaque to visible light and results in a white film on the skin[14]. Currently, sun protection properties have been improved by reducing the particle size of zinc oxide and titanium dioxide from microscale to nanoscale to have more transparent without losing their ability to screen UV rays.

There are many studies that support the advantages of nano-size inorganic active ingredient. Gasparro et al.[11] (1998) reported that when the average particle size of metal oxides is reduced below the optimum light scattering size, allowing visible light transmission. This results in the invisibility of inorganic nanoparticles on the skin that now being widely used in sunscreen and skin care product. Morabito et al.[12] (2011) supported that these nano materials have higher UV absorbs and scatters than the bulk pigments. The illustrates of this effect are showed in Fig. 2-4.

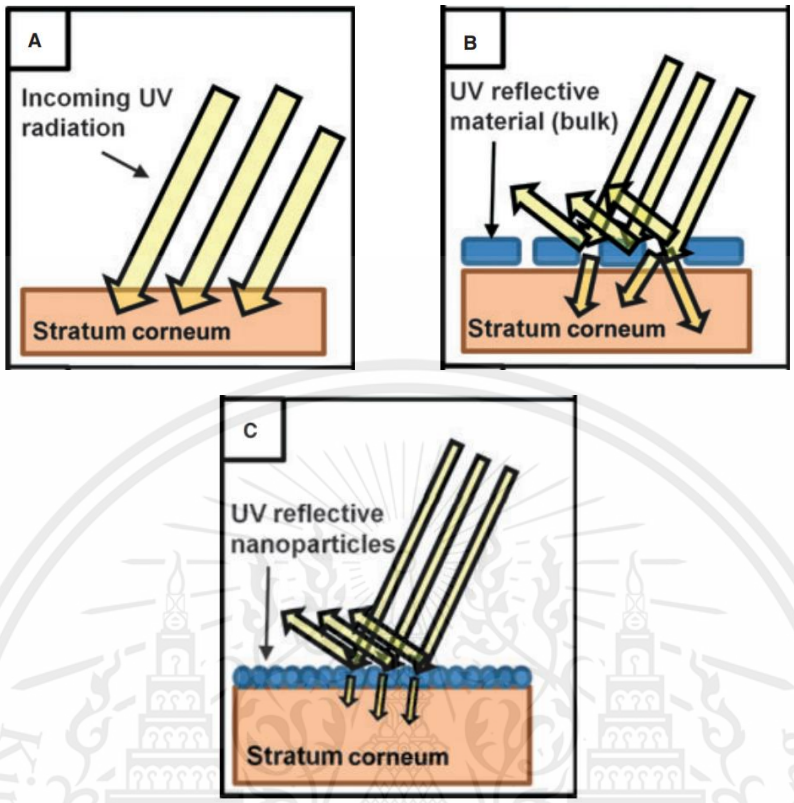

Figure 2-4 (A) Incoming UV radiation penetrates the stratum corneum. (B) UV reflective material in bulk form (e.g., ZnO) (C) UV reflective nanoparticles (e.g., ZnO).
Adapted from Morabito, K.; Shapley, N. C.; Steeley, K. G.; Tripathi, A. Review of Sunscreen and the Emergence of Non-Conventional Absorbers and Their Applications in Ultraviolet Protection. *Int. J. Cosmet. Sci.* 2011, *33*, 385–390. https://doi.org/10.1111/j.1468-2494.2011.00654.x.

Smijs and coworker[17] (2011) supported that micro-size reduction of ZnO and TiO_2 increases the UVB absorption of both particles, with the expense of UVA-I absorption, resulting in the unbalanced of UV protection. This problem could be solved by combination of various microsized ZnO particles and nanosized TiO_2.

In sunscreens, TiO_2 and ZnO is often coated with silicon oil, SiO_2 or Al_2O_3 to enable more usability with organic ingredients and improve UV dispersion and absorption in the overall formulation. ZnO is a better sunscreen ingredient than TiO_2 because of its more transparent and covers a broader UVA spectrum. Alternatively, TiO_2 is considered superior because it provides a much higher SPF than ZnO. Dunford et al.[18] (1997) supported that TiO_2 particle in sunscreen are often coated with compounds (such as alumina, silica, zirconia) that form hydrated oxides which can capture hydroxyl radicals and may reduce photosensitivity.

The inorganic ingredient used in sunscreens are favorable because of its absorption, reflection and scattering of UV radiation. It has a broad spectrum of coverage. Therefore, adding inorganic ingredient can minimize the amount of organic ingredients needed that will be helpful for people with sensitive or skin irritation.

The increased use of inorganic UV sunscreens is due to the low irritant reactions. In combination with organic sunscreen, TiO_2 provides impressive SPF and showed broad absorption in both UVB and UVA regions.

The disadvantage of using inorganic components as sunscreen agents is its dispersion that require additional materials to coat inorganic materials. Coatings are also used to reduce the photoreactive of inorganic components and protect the potential risk of free radical formation through oxidation when inorganic components exposed to UV rays.

2.2 Titanium dioxide

TiO_2 or titania is metal oxide of titanium that naturally occurring compound occurred when titanium reacts with oxygen in the air. It has high refractive index which ability to scatter light and absorb UV rays[19]. TiO_2 has white color, which act as white pigment several industries[20]. TiO_2 is dielectric material that chemically stable and non-toxic[21].

TiO_2 NPs are used in many industries such as photocatalysis, antibacterial agent, Nano-paint[22], food industry, orthodontic composites, air purification and solar cells[23]. In part of food industry, it is used to increase the sheen of food[24]. In cosmetic industry, it is also commonly used as an important ingredient in protective agents in physical sunscreen because of the properties of UV protection over a wide wavelength covers both UVA and UVB rays and is more effective in UVB protection than zinc oxide.

There are three crystalline form: rutile, anatase and brookite. Rutile is the more common form of titania although anatase is the more stable form. In sunscreen, rutile is commonly used but anatase is commonly use in photocatalysis. The main difference between rutile and anatase is anatase is more photoactive form of TiO_2[25]. Auger and Martinez[26] (2009) reported rutile TiO_2 has refractive index of 2.8 that is an effective pigment for use as white coating. The high refractive index for all crystalline TiO_2, resulting in good scattering properties and whiteness. TiO_2 in micronize form tend to form larger clusters, opaque will occur, and it can reduce its photoprotection efficacy[27]. Therefore, several studies have tried to solve these problems by coat the TiO_2 particles with silica. Silica-based coatings are used to reduce photocatalytic effects and helpful for UVB absorption. Morphology and particle size affect the optical properties of TiO_2 that is these factors were controlled to develop sun protection properties.

In the present, modified TiO_2 nanoparticles were studied and synthesized to enhance its properties such as hollow TiO_2 spheres, surface coating of TiO_2, TiO_2 nanofibers, TiO_2 nanowire, TiO_2 nanorods, TiO_2 nanosheet and mesoporous TiO_2[28]. While modified TiO_2 nanoparticles is being developed for many applications, the structure that

has received a lot of attention is hollow TiO_2 nanoparticles because of its properties, such as having a large surface area, low density and has a greater light scattering[29]. El-Toni et al[30] (2015) reported that if we compare between the same size of dense and hollow spheres, Hollow morphology is more efficient as a catalyst because of its outer and inner surfaces can more react with the reactants than dense morphology. Example of modified TiO_2 nanoparticles studied in field of dye-sensitized solar cell, Mustafa et al.[31] (2019) reported polyvinyl-alcohol/titanium dioxide (PVA/TiO_2) nanofibers are used as a light scattering layer (LSL) on top of the TiO_2 nanoparticles photoanode showed higher power conversion efficiency (PCE) than TiO_2 nanoparticles without LSL because it reduced the radiation loss and increase the excitation of the electron, resulting in more power conversion efficiency to be generated as showed in Fig. 2-5.

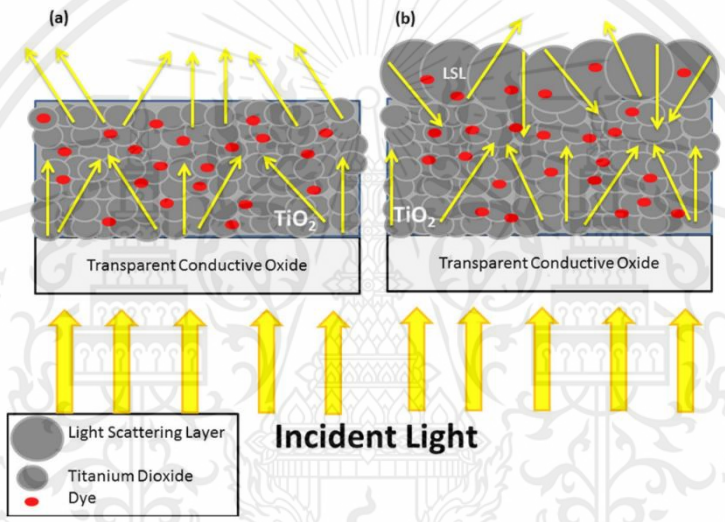

Figure 2-5 Illustration of light loss of (a) photoanode without light scattering layer and (b) photoanode with light scattering layer.
Adapted from Mustafa, M. N.; Shafie, S.; Wahid, M. H.; Sulaiman, Y. Light Scattering Effect of Polyvinyl- Alcohol / Titanium Dioxide Nanofibers in the Dye-Sensitized Solar Cell. *Sci. Rep.* 2019, *9*, 1–8. https://doi.org/10.1038/s41598-019-50292-z.

In addition to modified TiO_2 particles to enhance UV protection properties. There are also modified TiO_2 particles for compatibility with organic materials. Li et al.[32] (2019) have synthesized lignin colloidal spheres encapsulated TiO_2 (LCS@TiO_2) to improve the compatibility with hydrophobic cream. The resulted showed that the LCS encapsulated TiO_2 has a water contact angle as high as 89° in comparison to only 22° in the TiO_2 disk control sample as showed in Fig. 2-6.

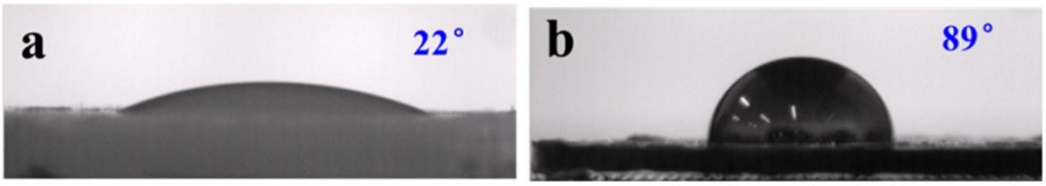

Figure 2-6 Wettability of water droplet on the surfaces of (a) TiO_2 and (b) LCS@TiO_2-2 disks.
Adapted from Li, Y.; Yang, D.; Lu, S.; Qiu, X.; Qian, Y.; Li, P. Encapsulating TiO_2 in Lignin-Based Colloidal Spheres for High Sunscreen Performance and Weak Photocatalytic Activity. *ACS Sustain. Chem. Eng.* 2019, *7*, 6234−6242 Research. https://doi.org/10.1021/acssuschemeng.8b06607.

Studied of penetration of nanoparticles, Lademann et al.[2] (2011) reported TiO_2 nanoparticles in sunscreens can penetrate the human stratum corneum and can be found in some hair follicles including deeper parts but penetration of TiO_2 particles into living tissue could not be observed. His investigation performed by means of tape stripping and X-ray fluorescence technique. Nakagawa et al.[33] (1997) reported that the photoexcited TiO_2 particles cause primary DNA damage and structural chromosome aberrations in cultured mammalian cells that depend on dose of TiO_2 and UV-vis light intensity. Fig 2-7 showed effect of photoexcited TiO_2 on U937 cells, the ultrafine TiO_2 particles without light irradiation showed little toxicity to living cell resulting in greater than 90% of the surviving fraction. While 20% of cell were damaged because of UV light without TiO_2. When TiO_2 exposed UV light, all cells were damaged after 30 min irradiation. However, there are some studied that investigated about the potential for DNA damage related to the use of titanium dioxide inorganic UV filters in sunscreens. Huang et al. [34] (1997) reported that an uncoated 10 nm TiO_2 irradiated by UVA and UVB can causes oxidative damage to DNA.

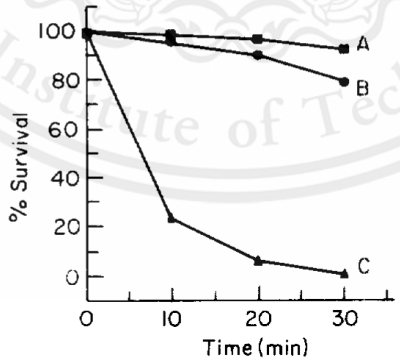

Figure 2-7 Effect of light and TiO_2 on the viability of U937 cells: (a) TiO_2 (1000 $\mu gm1^{-1}$) in the dark; (b) no TiO_2 in the light; (c) TiO_2 (1000 $\mu gm1^{-1}$) in the light.
Adapted from Huang, N.; Xu, M.; Yuan, C.; Yu, R. The Study of the Photokilling Effect and Mechanism of Ultrafine TiO_2 Particles on U937 Cells. *J. Photochem. Photobiol. A Chem.* 1997, *108*, 229–233.

The use of titanium dioxide (TiO_2) particles as a sunscreen ingredient raises concerns about the potential risks of the generation of $HO^{\bullet}$ and $O_2^{-\bullet}$ radicals along with other reactive oxygen species (ROS), including H_2O_2 that can potentially damage to biomolecules**.** Moreover, whether TiO_2 penetrates the skin or not but hydrogen peroxide and oxygen can penetrate the skin[35]. At present, the efforts have been focused on reducing the yield of free radical generation by TiO_2 when exposed to sunlight by coating of titanium dioxide particles[36].

2.3 Literature reviews

Light scattering and reflections of particles are important properties for many ways such as photocatalytic activity, architectural coatings, dye-sensitized solar cell, and sunscreen.

There are many studies support that morphology affect to optical properties of particles. Thiwakornkitkul and Suteewong[8] (2019) reported that hollow TiO_2 nanoparticles showed higher reflectance than dense TiO_2 nanoparticles. Hollow cavity allows light scattering and reflection that can enhance photocatalytic activity. In addition, band gap energy of hollow TiO_2 NPs has slightly higher than dense TiO_2 as showed in Fig. 2-8.

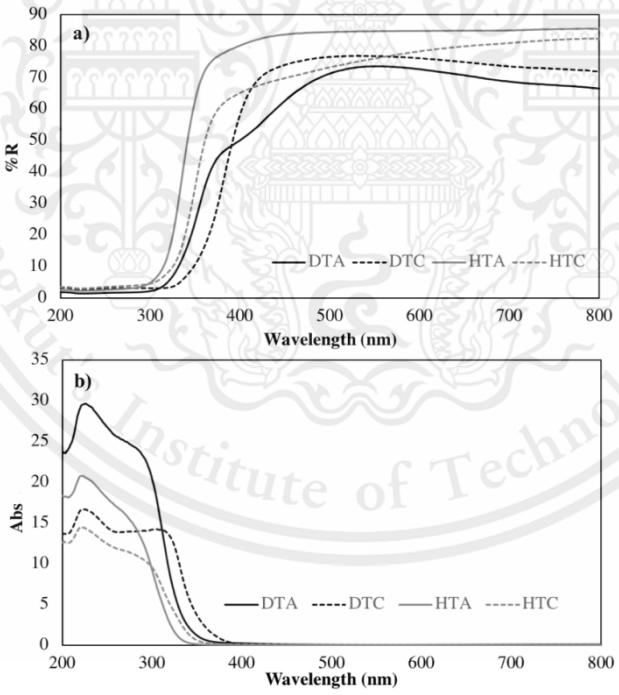

Figure 2-8 UV-DRS spectra of (a) %reflectance (%R) and (b) absorbance (Abs) of amorphous dense TiO_2 (DTA), amorphous hollow TiO_2 (HTA), calcined dense TiO_2 (DTC) and calcined hollow TiO_2 (HTC), respectively
Adapted from Thiwakornkitkul, N.; Suteewong, T. Effect of Morphology of Titanium Dioxide Nanoparticles on Photocatalytic Activity. IOP Conf. Ser. Mater. Sci. Eng. 2019, 639 (1). https://doi.org/10.1088/1757-899X/639/1/012021.

Lu Ren et al.[29] (2020) prepared TiO_2 hollow nanoparticles with tunable cavity size. The results show the larger cavity of the TiO_2 hollow nanoparticles with anatase, and rutile mixture phases (TiO_2-3HF) has stronger UV absorption than a smaller dominant cavity size (TiO_2-1.5HF) and the TiO_2 solid nanoparticles (TiO_2-0HF). In contrast, the larger cavity of the TiO_2 hollow nanoparticles with pure anatase phase, has lower the UV absorption as showed in Fig. 2-9. They supported that hollow TiO_2 nanoparticles have unique structure and cavity-size-dependent properties.

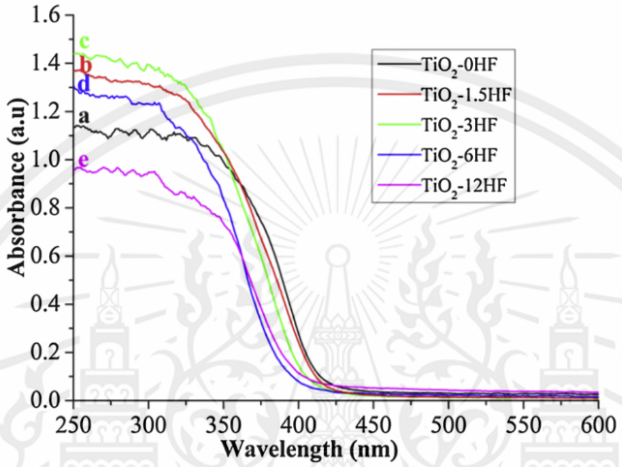

Figure 2-9 Diffusive reflectance UV–vis absorption spectra of TiO_2 samples: (a) TiO_2-0HF, (b) TiO_2-1.5HF, (c) TiO_2-3HF, (d) TiO_2-6HF and (e) TiO_2-12HF.
Adapted from Ren, L.; Li, Y.; Hou, J.; Wang, T.; Yang, Y.; Zhao, X. Fabrication and Cavity-Size-Dependent Photocatalytic Property of TiO_2 Hollow Nanoparticles with Tunable Cavity Size. Mater. Res. Bull. 2020, 126 (December 2019), 110744. https://doi.org/10.1016/j.materresbull.2019.110744.

Auger and McLoughlin[37] (2014) reported that the air layer around TiO_2 pigment that bounded by a hard polymer is enhance the scattering efficiency due to an increase in the refractive index difference between TiO_2 pigment and its surrounding medium as showed in Fig. 2-10. In part of rattle core–shell titania microspheres, they also believed that suitable core size is allowed multiple light reflections within the cavity, which improve enhance the photocatalytic activity[37].

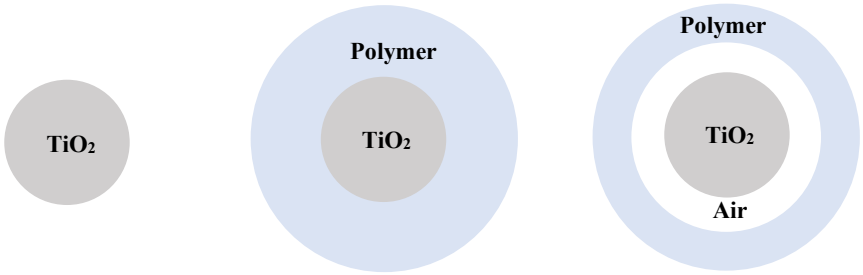

Figure 2-10 Three different types of particles under study.
Adapted from Auger, J.; Mcloughlin, D. Theoretical Analysis of Light Scattering Properties of Encapsulated Rutile Titanium Dioxide Pigments in Dependent Light Scattering Regime. Prog. Org. Coatings 2014, 77 (11), 1619–1628. https://doi.org/10.1016/j.porgcoat.2014.05.005.

Gupta et al.[21] (2013) reported that the shape, size, and spatial arrangement of the particles can affect light scattering. His team used titanium dioxide nanoparticles to create multiple reflections and strong light scattering from the difference in the optical properties between the TiO_2 particles and air.

Dadgostar et al.[38] (2012) synthesized the mesoporous structure of the TiO_2 hollow sphere that provides a high surface area of 74 m^2/g which allows for higher dye loading. This suggests that the TiO_2 hollow sphere could be a good substitute for common TiO_2 spheres as a scatterer in DSC. Fig. 2-11 showed the dye loading on TiO_2 filled sphere (T-FS cell) is more than the single transparent film (T) about 10%. While the dye loading on TiO_2 hollow sphere (T-HS cell) is more than the single transparent film (T) about 40%. Thus, T-HS cells is better in the loading of the absorbing dyes.

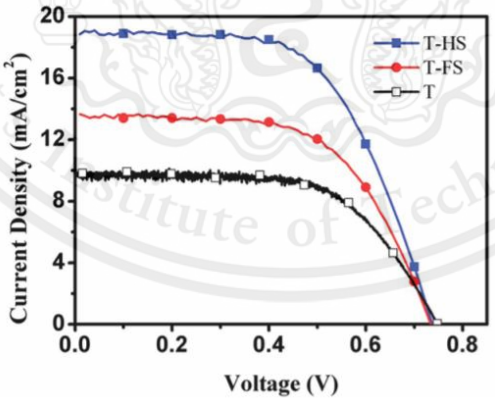

Figure 2-11 I–V curves of DSCs with a photoanode of a single transparent film (T) without a scattering layer, and with filled sphere (FS) and hollow sphere (HS) scattering layers.
Adapted from Dadgostar, S.; Tajabadi, F.; Taghavinia, N. Mesoporous Submicrometer TiO_2 Hollow Spheres As Scatterers in Dye-Sensitized Solar Cells. *ACS Appl. Mater. Interfaces* 2012, *4*, 2964–2968. https://doi.org/dx.doi.org/10.1021/am300329p.

Hee Jung Kim et al.[39] (2019) have synthesized SiO_2 coated platy TiO_2 (S-pTi) as a noble UV/IR-shielding material. It was found that particle shape and size are affect to IR reflectance. The pTi showed higher reflectance than nTi at longer IR wavelengths and all SiO_2 coating samples still maintain high reflectance that means the S-pTi with large plate form can prevent the IR heat source into the skin because of its wide shielding area. These results showed that the S-pTi sample has potential applications in UV and heat-protection materials.

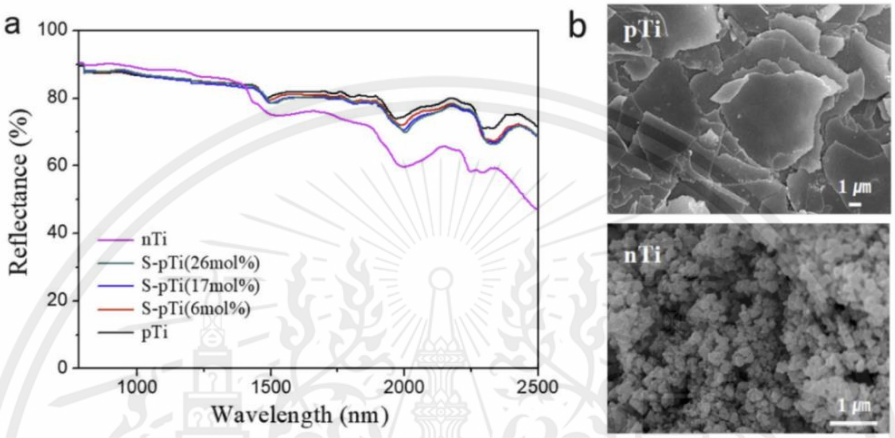

Figure 2-12 (a) NIR reflectance spectra of nTi and S-pTi samples; and (b) FE-SEM images of pTi and nTi.
Adapted from Kim, H. J.; Roh, D. K.; Chang, J. H.; Kim, D. SiO_2 Coated Platy TiO_2 Designed for Noble UV/IR-Shielding Materials. *Ceram. Int.* 2019, *45* (May), 16880–16885. https://doi.org/10.1016/j.ceramint.2019.05.231.

Wang et al.[9] (2017) have synthesized bio-inspired dopamine-melanin solid nanoparticles (Dpa-s NPs) and hollow nanoparticles (Dpa-h NPs) as UV-absorbers in polymer. The results showed that Dpa-h NPs have higher efficiency for UV-shielding performance because the holes of the Dpa-h NPs allow UV light to shine inside the hollow structure and make it difficult for the UV light to escape. After multiple reflections and absorption inside the hollow nanoparticles, the UV light is captured and absorbed by the Dpa-h NPs finally. The UV-shielding mechanisms are showed in Fig 2-13.

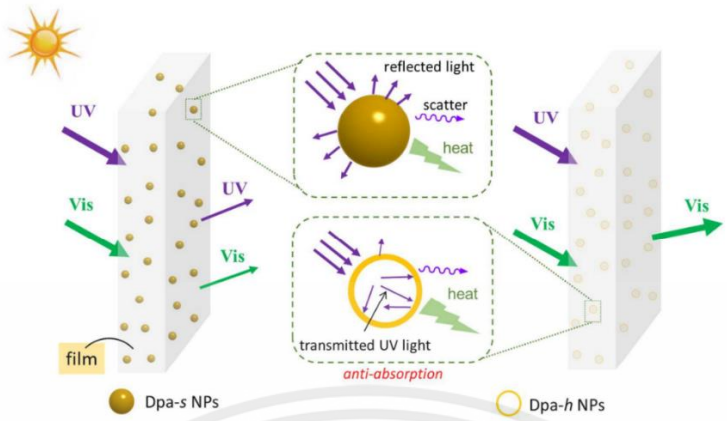

Figure 2-13 The illustration of the UV-shielding mechanisms of PVA/Dpa-s and PVA/Dpa-h nanocomposites, respectively.
Adapted from Wang, Y.; Su, J.; Li, T.; Bai, H.; Xie, Y.; Chen, M.; Dong, W. A Novel UV-Shielding and Transparent Polymer Film : When Bio-Inspired Dopamine-Melanin Hollow Nanoparticles Join Polymer. *ACS Appl. Mater. Interfaces Mater. Interfaces* 2017. https://doi.org/10.1021/acsami.7b08763.

Sudjaipraparat, Kaewsaneha, Nuasaen, and Tangboriboonrat[40] (2017) synthesized non-spherical (ns) hollow latex (HL) particle with a void on one side of a polymer particle surrounded by a double-layered shell via the one-pot seeded emulsion polymerization (SEP). They reported that coating containing HL particles has higher opacity value because the refractive index (Δn) that is different between the inner P(St/AA) shell and the outer P(DVB/MMA/AA) shell of HL particle scatter the incident light twice before reaching the air void resulting the multiple light scattering.

Sukanya Nuasaen and Pramuan Tangboriboonrat [41] (2015) synthesized poly(methyl methacrylate-co-divinyl benzene-co-acrylic acid) (P(MMA/DVB/AA)) hollow latex particles or the poly(styrene-co-acrylic acid) (P(St/AA)) and poly(styrene-co- methyl methacrylate-co-acrylic acid) (P(St/MMA/AA)) solid particles, used as white pigment in paint film. They reported that the film containing HL particles, allowing multiple light scattering, showed better hiding efficiency compared to coatings containing solid particles as shown in Fig 2-14.

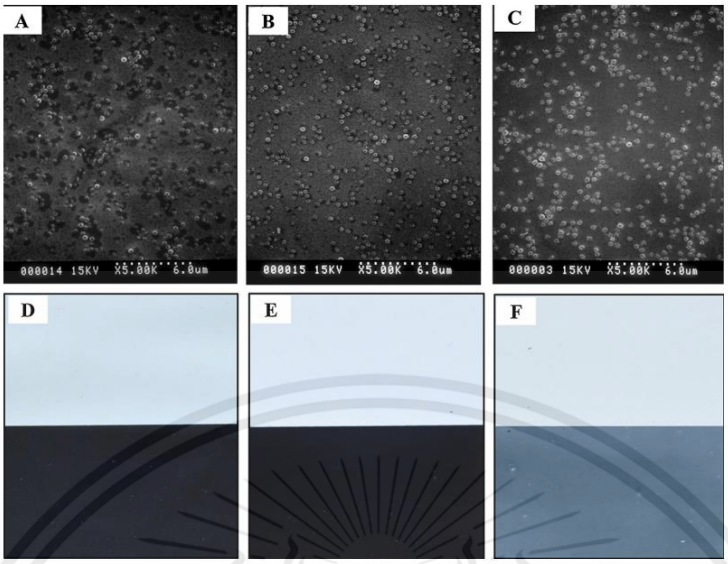

Figure 2-14 SEM images of coatings formulated with P(St/AA) (A), P(St/MMA/AA) (B), and HL (C) particles and the corresponding image showing hiding power on black and white chart papers for each coating (D–F).
Adapted from Nuasaen, S.; Tangboriboonrat, P. Optical Properties of Hollow Latex Particles as White Pigment in Paint Film. *Prog. Org. Coatings* 2015, *79* (C), 83–89. https://doi.org/10.1016/j.porgcoat.2014.11.012.

Chava et al.[42] (2017) synthesized hollow TiO_2 NPs (H-TiO_2) as a light scattering layer in dye-sensitized solar cells (DSSCs). They reported that DSSCs based on H-TiO_2 photoanodes revealed more dye absorption compared to that of C-TiO_2 NPs, confirmed that the enhanced photovoltaic efficiency (η) of the DSSCs fabricated from H-TiO_2 NPs is closely related with the larger amounts of anchored dye molecules. The reflecting and scattering of light in a H-TiO_2 NP showed in Fig. 2-15a. They supported that the improved photocurrent for the H-TiO_2 NPs is contributed to by its hollow spherical structure which provides way to enhance light-harvesting efficiency. Moreover, the overall IPCE increases by the introduction of a scattering layer, and the H-TiO_2 films possess higher IPCE values than the C-TiO_2 NP film over the whole spectral range as showed in Fig. 2-15b.

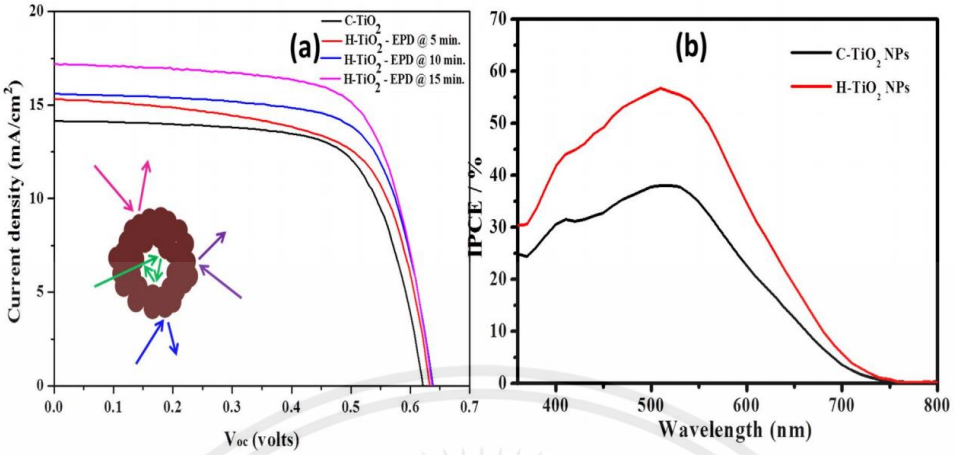

Figure 2-15 (a) I-V characteristics of DSSCs assembled with the C-TiO_2 screen printed and bi-layer structure with H-TiO_2 films of varying thicknesses, (b) IPCE spectra of DSSCs made from C-TiO_2 film and bilayer structure with H-TiO_2 NPs. Adapted from Rama Krishna, C.; Lee, W. M.; Oh, S. Y.; Jeong, K. U.; Yu, Y. T. Improvement in Light Harvesting and Device Performance of Dye Sensitized Solar Cells Using Electrophoretic Deposited Hollow TiO_2 NPs Scattering Layer. Sol. Energy Mater. Sol. Cells 2017, 161 (November 2016), 255–262. https://doi.org/10.1016/j.solmat.2016.11.037.

CHAPTER III

RESEARCH METHODLOGY

3.1 Chemicals

1) Tetraethyl orthosilicate (TEOS, ≥99.0%), Aldrich
2) Titanium tetraisopropoxide (TTIP, ≥99.0%), Aldrich
3) Titanium tetrabutoxide (TBT, ≥97.0%), Aldrich
4) Methanol
5) Ethanol ≥99.0% (AR), RCI Labscan
6) Ammonium Hydroxide, Ammonia Solution 30% for analysis, PanReac
7) Deionized water (DI water)
8) Sodium hydroxide (NaOH (s), 99%), Fluka
9) Calcium chloride ($CaCl_2$, 75%), Chemipan

3.2 Apparatus

1) Round-bottom flasks
2) Erlenmeyer flasks
3) Graduated Cylinders
4) Volumetric flasks
5) Beakers
6) Hot plate stirrer
7) Stand and clamp
8) Pipette and micropipette
9) Dropper
10) Oven
11) Sonicator
12) Centrifuge tube
13) Centrifuge machine
14) Condenser column
15) Rubber strap
16) Glass Stopper
17) Spatula
18) Analytical balance
19) Magnetic bar
20) Grease

3.3 Experimental

3.3.1 Synthesis of SiO_2 core nanoparticles

1) Ethanol and ammonium hydroxide were first mixed in an Erlenmeyer flask for 10 minutes.
2) Add TEOS into the prepared solution and stir for 1 hour.
3) Add 17 μL of TEOS into the mixture every 5 minutes for ten times and stir for 8 hours.
4) Remove the excess chemicals by centrifugation at the speed of 10,000 rpm for 10 minutes. The silica nanoparticles were redispersed in ethanol. Then, repeat the washing step again.
5) Various of silica precursor (TEOS) and catalyst (NH_4OH) were added to adjust particle size.

3.3.2 Synthesis of hollow TiO_2 nanoparticles

Method I[43]

1) The prepared SiO_2 nanoparticles in ethanol was dispersed in a mixture of ethanol, acetone, and ammonia solution.
2) Stir for 30 minutes at 85°C (refluxing conditions) and room temperature to vary reaction temperature.
3) Adding various volumes of TBT solution into the refluxed solution to adjust shell thickness and particle size.
4) The solution was further stirred for 2 hours at refluxing conditions.
5) The SiO_2@TiO_2 core-shell particles were collected by centrifugation at 10500 rpm and then washed several times with ethanol and DI water.
6) Add sodium hydroxide solution into the particle mixture and stir for 6 hours to remove the silica cores.
7) Hollow particles were collected by centrifugation at 10500 rpm and then washed several times with DI water.

Method II[44]

1) Weigh the prepared SiO_2 nanoparticles that dispersed in ethanol.
2) Disperse SiO_2 NPs in ethanol in a mixture of DI water and ethanol. Stir for 30 minutes.
3) While the temperature was increased to 85°C. Prepare the solution of titanium tetrabutoxide in ethanol at various volume ratio.
4) Inject titania precursor into the refluxed solution at a rate of 0.5 mL/min.
5) Stir under refluxing conditions for 100 min.
6) Remove unreacted chemicals by centrifugation, wash with ethanol and re-disperse the SiO_2@TiO_2 core-shell particles in DI water.
7) Add sodium hydroxide solution into the particle mixture and stir for 6 hours before cleaning with DI water.

8) Hollow particles were collected by centrifugation at 10500 rpm and then washed several times with DI water and ethanol. Re-disperse the hollow TiO_2 NPs in DI water.

3.3.3 Synthesis of dense TiO_2 nanoparticles[45]

1) Firstly, 50 mL MeOH was added in a round-bottom flask.
2) Add 200 μL of different concentrations of $CaCl_2$ solutions into MeOH and stir for 10 minutes.
3) 850 μL of TTIP was added dropwise.
4) The resulting solution was stirred for 24 h at room temperature.
5) The synthesized TiO_2 nanoparticles were collected by centrifugation at 10500 rpm and then washed several times with ethanol and DI water.

3.4 Characterization

The synthesized dense and hollow titanium dioxide nanoparticles will be characterized by Transmission Electron Microscopy. Particle size and shell thickness of particles were measured by TEM using JEM-2100 Electron Microscope and Particle Analyzer using Delsa Nano C of Beckman Coulter.

Chapter IV

Results and Discussion

4.1 Synthesis of SiO_2 nanoparticles

Spherical silica nanoparticles (SiO_2 NPs) having an average size from 30 to 270 nm were synthesized via Stöber method. Particle size of SiO_2 NPs was controlled by varying amounts of the silica precursor (TEOS) and catalyst (NH_4OH). In this study, at ca. 80-130 nm SiO_2 NPs were used as core for titania coating.

4.1.1 Effect of TEOS concentration

Fig. 4-1 shows TEM images of spherical SiO_2 NPs obtained by controlling the TEOS concentrations. The results that showed, average particle size from TEM analysis increased from 114.09±11.14 nm to 262.37±14.86 nm with increasing concentration of TEOS from 0.08 to 0.10 M because rate of hydrolysis and condensation become higher.

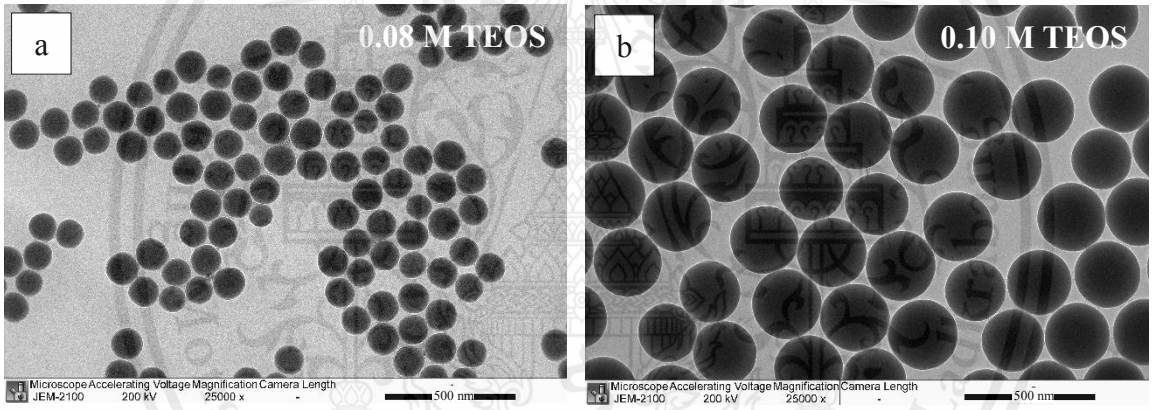

Figure 4-1 TEM images of spherical SiO_2 NPs obtained by adjusting concentrations of TEOS. Average sizes by JEM-2100 Electron Microscope are (a) 262.37±14.86 nm (b) 114.09±11.14 nm, measured by ImageJ.

Fig. 4-2 shows hydrodynamic size of silica particles by number distribution at various concentrations of TEOS. As concentrations of TEOS increase from 0.035 to 0.084 M, the average particle size increased from 120.76±8.64 nm to 162.80±5.96 nm. The results showed that when the concentration of TEOS were increased, average particle size increased due to increasing hydrolysis and condensation rate.

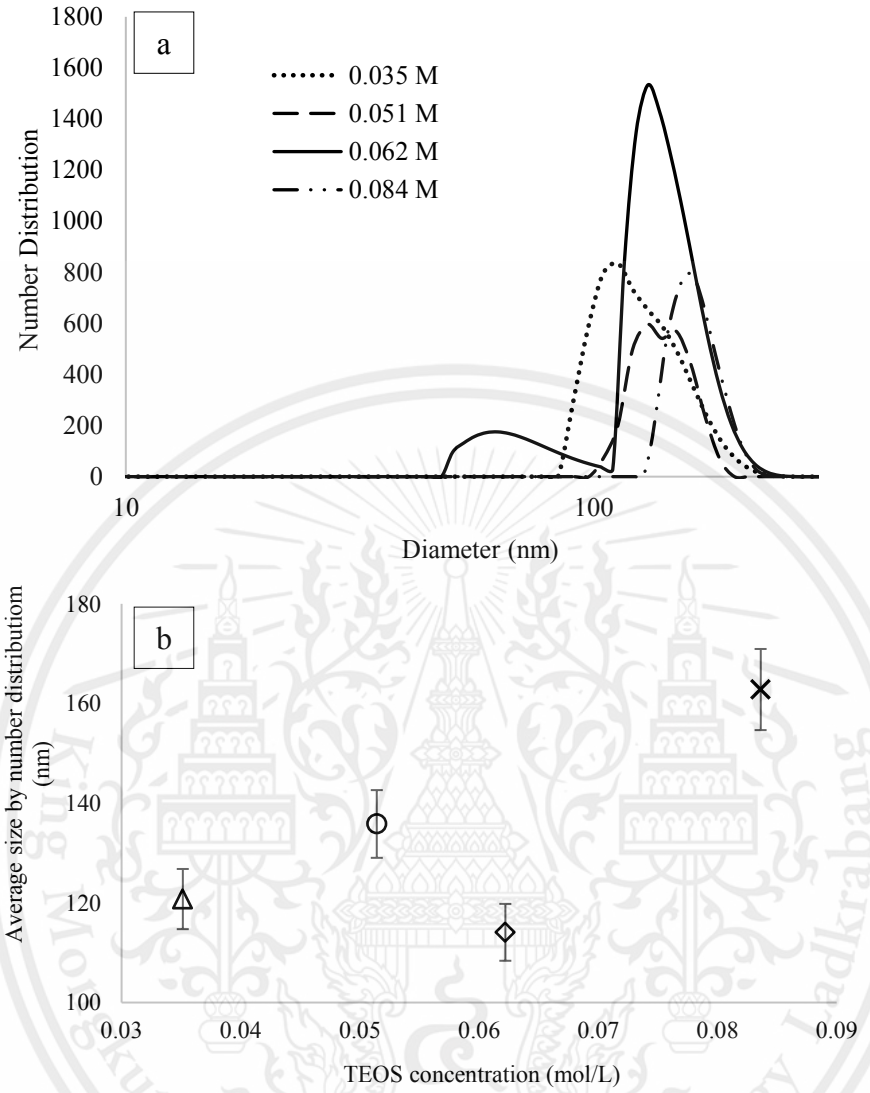

Figure 4-2 (a) average particle size by number distribution (nm) at TEOS concentrations from 0.035 to 0.084 M, measured by DLS. (b) graph shows relation between average particle size by number distribution (nm) and effect of TEOS concentration (M). Average size by number distribution using Particle Analyzer, Delsa Nano C of Beckman Coulter.

TEOS is silica precursor in hydrolysis and condensation in the Stöber process, which hydrolyzes to generate siloxane molecules and ethanol. Then the condensation polymerization occurs through the siloxane molecules and TEOS molecules or siloxane molecules themselves, which relate to the final size and uniformity of the nanoparticle. This trend is consistent with work of Ren et al.[46] They reported that the average size of particles increased with the increase of TEOS concentrations. Rates of hydrolysis and condensation were accelerated by increasing the concentration of TEOS.

4.1.2 Effect of NH_4OH concentration

Fig. 4-3 shows hydrodynamic size of silica particles by number distribution at various NH_4OH concentrations. Average particle sizes increased from 51.05±4.40 nm to 128.39±23.05 nm, when NH_4OH concentrations increased from 0.202 to 0.297 M at 0.063 M TEOS. As concentrations of NH_4OH increase from 0.202 to 0.297 M at 0.036 M TEOS, the average particle size increased from 42.71±1.18 nm to 120.76±8.64 nm.

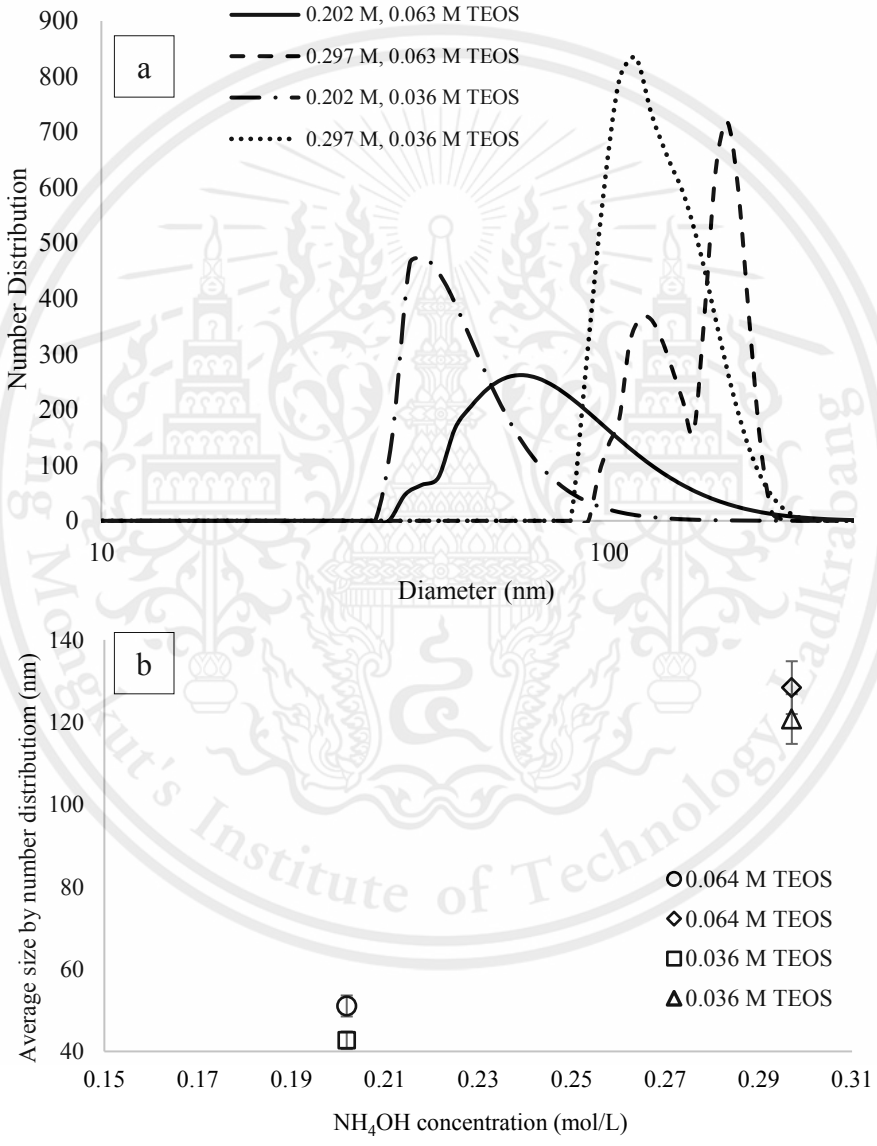

Figure 4-3 (a) Average particle size by number distribution (nm) at NH_4OH concentrations from 0.202 to 0.297 M, at 0.036 and 0.063 M TEOS, measured by DLS. (b) graph shows relation between average particle size by number distribution (nm) and effect of NH_4OH concentration (M). Average size by number distribution using Particle Analyzer, Delsa Nano C of Beckman Coulter.

Regardless of TEOS concentration, particles size increased with increasing of catalyst concentration because rate of hydrolysis and condensation become higher. The results showed that the particle size was increased by increasing the NH_4OH concentration. Ammonium hydroxide act as catalyst for hydrolysis and condensation of TEOS. The higher NH_4OH concentration attribute to the higher pH and hydrolysis rate, which consistent with work of Park, Sung Kyoo et al.[47] Matsoukas and Gulari[48] supported that the effect of ammonia concentration is to promote hydrolysis, but also to promote the condensation rate, resulting in faster kinetics, and larger particles sizes. In addition, Ren et al.[46] reported that the rate of hydrolysis was influenced by the concentration of basic catalyst. The nucleus is quickly forming, causing particles to grow uniformly. This trend was consistent with work of Kim et al.[49]

4.2 Synthesis of hollow TiO_2 nanoparticles

Hollow TiO_2 NPs with various particle diameter and shell thickness were synthesized via two different sol-gel method, using 262.37±14.86 nm, measured by TEM and 128.39±23.06 nm, measured by DLS as core for titania coating.

4.2.1 Synthesis of hollow TiO_2 nanoparticles method I

Fig. 4-4 shows TEM images of different SiO_2 NPs core size before (Fig. 4-4(a, c)) and after coating (Fig. 4-4(b, d)). With ca. 262.37±14.86 nm SiO_2 NPs surface before coating was smooth (Fig. 4-4(a)). After coating with TBT concentration of 8.11 mM, particle size become larger (351±40.08 nm) and surface become rougher (Fig. 4-4(b)). The results indicate the presence of 45-nm TiO_2 layer on SiO_2 NPs. Their average sizes were measured using ImageJ. At ca. 30-nm SiO_2 NPs (Fig. 4-4(c)) were coated with the same concentration of TBT, aggregated titania-coated silica NPs (SiO_2@TiO_2 core-shell NPs) were observed (Fig. 4-4(d)). As a result of excess or non-optimum of titania precursor, particle size and amount of SiO_2 core.

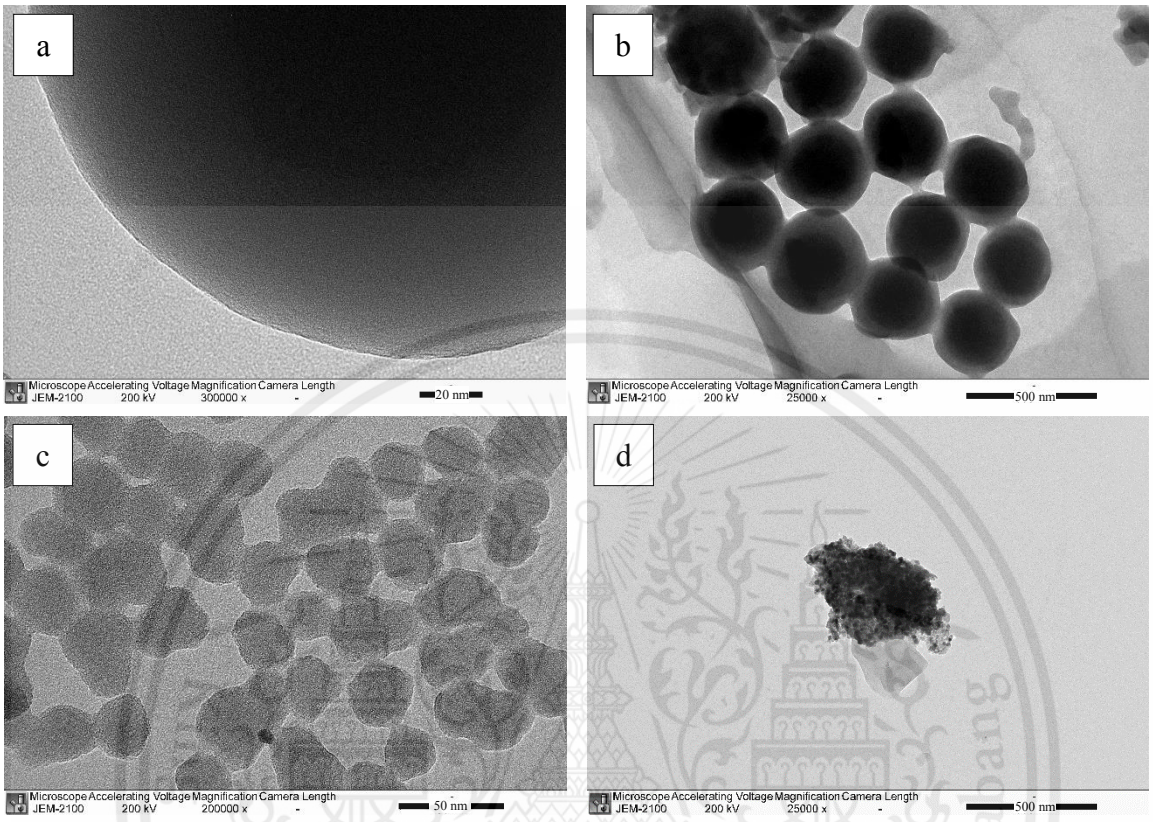

Figure 4-4 TEM images of (a) 260-nm SiO_2 NPs surface (b) 350-nm SiO_2@TiO_2 core-shell NPs (c) 30-nm SiO_2 NPs and (d) aggregated SiO_2@TiO_2 core-shell NPs were synthesized at the same 8.11 mM of TBT concentration, at room temperature. Average size measured by ImageJ.

Figure 4-5 showed SiO_2 cores were successfully removed after etching. h-TiO_2-4.87 and h-TiO_2-8.11 NPs in Fig. 4-5(a) and (b) were synthesized at the same reaction temperature (room temperature) but used 128.39±23.06 nm SiO_2, measured by DLS as core. When increasing TBT concentration from 4.87 to 8.11 mM, particle size slightly increased from 129.87±8.07 to 133.93±8.68 nm, respectively. The shell thickness also increases. So, the TBT concentration of 4.87 mM was then selected to study effect of temperature. Fig.4-5(c) show morphology of h-TiO_2-4.87 NPs prepared at 85^{o}C but using the same titania precursor concentration and silica core. The results showed at higher reaction temperature, TiO_2 shell was smoother and slightly thicker (130.10±7.49 nm with approx. 15.15 nm shell thickness). Also, hollow structure maintained the spherical shape because when the temperature increased, condensation rate increased, resulting in more titanium dioxide deposited or coated on the silica core. The h-TiO_2-4.87 prepared at room temperature (Fig. 4-5(a)) performed thin shell. When SiO_2 cores were removed, deformation of particle was observed.

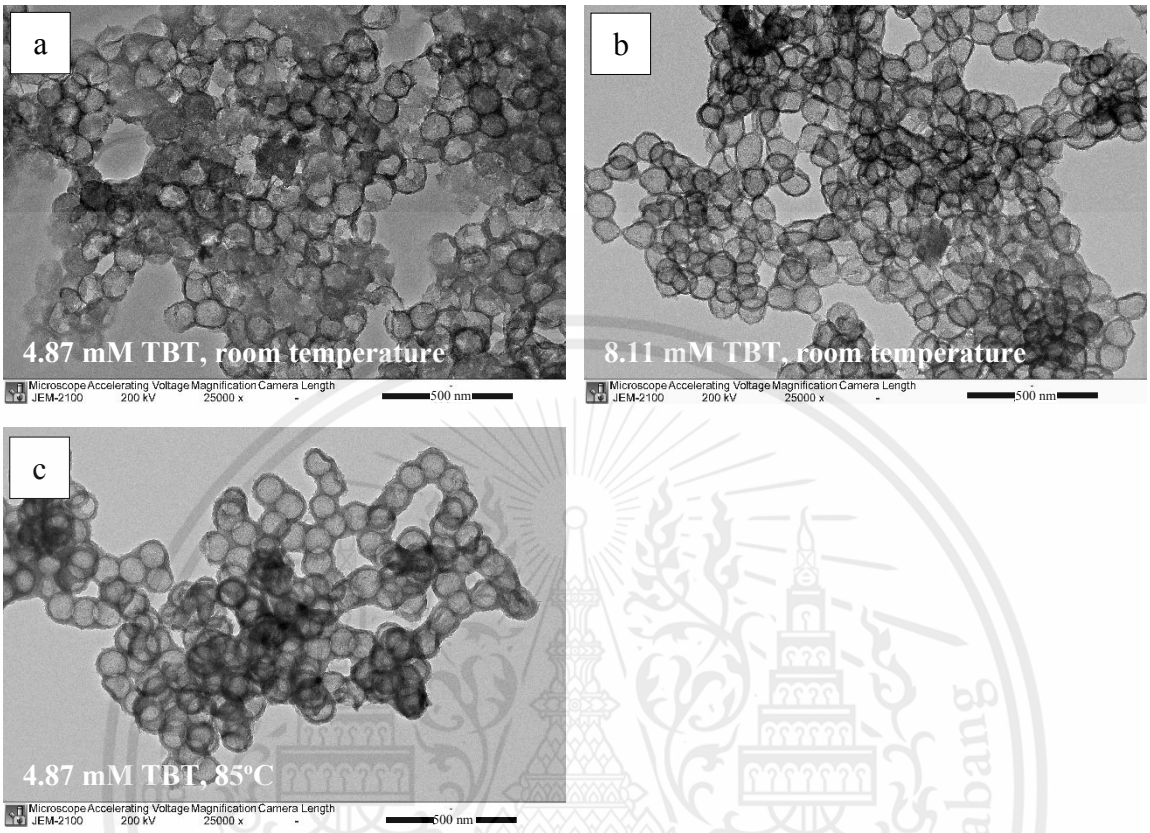

Figure 4-5 TEM images of (a) h-TiO_2-4.87 and (b) h-TiO_2-8.11 were synthesized at room temperature (c) h-TiO_2-4.87 were synthesized at 85ºC. Average size measured by ImageJ.

Hydrodynamic size of SiO_2@TiO_2 core-shell NPs were prepared by method I at TBT concentrations from 3.25 to 16.18 mM, at 85ºC were showed in Table 4-1. Light scattering measurement indicated that increasing of TBT concentrations led to the increase in particle size and shell thickness. The shell thickness of TiO_2 shell with varied from 20 to 50 nm were calculated by subtracting the size of silica core. Regardless of TBT concentration and temperature, resulting particles prepared from this protocol yielded aggregated particles, which may be the result of aggregation of silica particles before coating, excess amount of titania precursor in coating, or excessive concentrations of etching solution. However, not only the TBT concentration and temperature are important in coating, but the optimum amount of SiO_2 core is also important.

Table 4-1 Particle size and shell thickness of SiO_2@TiO_2 core-shell NPs synthesized at various TBT concentrations by method I at 85°C, analysed by DLS.

Sample	[TBT], mM	Particle size (nm)	Shell thickness (nm)
h-TiO_2-3.25	3.25	170.39±30.89	21.00±15.45
h-TiO_2-6.49	6.49	182.15±86.02	26.88±43.01
h-TiO_2-8.11	8.11	208.78±63.45	40.19±31.73
h-TiO_2-16.18	16.18	227.20±26.35	49.40±13.18

4.2.2 Synthesis of hollow TiO_2 nanoparticles method II

Fig. 4-6 shows TEM images of SiO_2@TiO_2 core-shell NPs synthesized by method II at 85°C, TBT: EtOH volume ratio of 2: 9 mL, before (Fig. 4-6(a)) and after (Fig. 4-6(b)) etching SiO_2 core. Size of SiO_2 core was 262.37±14.86 nm. Average particle size of SiO_2@TiO_2 core-shell NPs was approx. 296.56±13.03 nm. The results showed that large aggregate of h-TiO_2 were formed both before and after etching which may be the result of aggregation of silica particles before coating, excess amount of titania precursor in coating, or excessive concentrations of etching solution. After etching, some particles were fracture as showed at red arrows. However, their spherical shapes were still observed because the shell is significantly thick. The h-TiO_2 NPs prepared by method II at room temperature cannot observe after etching because of low temperature coating and lack of catalyst in reaction resulting in low condensation rate.

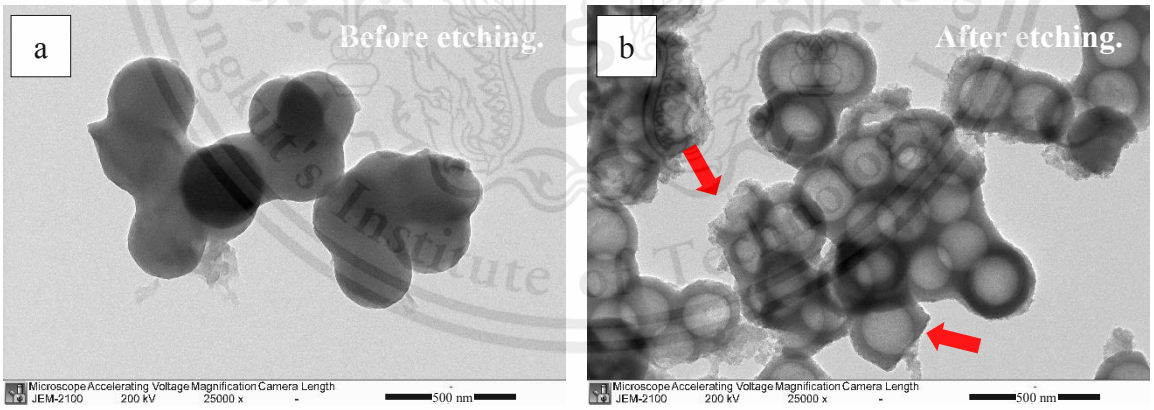

Figure 4-6 TEM images of SiO_2@TiO_2 core-shell NPs (a) before and (b) after etching, TBT: EtOH volume ratio of 2: 9 mL (95.96 mM TBT). These particles were synthesized via method II at 85°C. Average sizes were measured using ImageJ.

Hydrodynamic size of SiO_2@TiO_2 core-shell NPs were prepared by method II at TBT: EtOH volume ratio from 0.1:9 to 0.5:9, at 85°C. At ca. 130-nm SiO_2 were used as core, as presented in Table 4-2. The relevant concentrations of TBT were also in this Table.

Light scattering measurement indicated that particles size and shell thickness increased with increasing titania precursor concentration, similar trend with method I. Average particle size were in range of 150 to 460 nm. The shell thickness of TiO_2 shell were varied from 10 to 170 nm as showed in Table 4-2.

Table 4-2 Particle size and shell thickness of SiO_2@TiO_2 core-shell NPs synthesized at various volume ratio of TBT: EtOH by method II at 85ºC.

Sample	TBT (mL): EtOH (mL)	[TBT], mM	Particle size (nm)	Shell thickness (nm)
h-TiO_2-4.95	0.10: 9	4.95	150.06±20.76	10.84±10.38
h-TiO_2-9.89	0.20: 9	9.89	166.05±10.04	18.83±5.02
h-TiO_2-14.80	0.30: 9	14.80	274.19±66.18	72.90±33.09
h-TiO_2-19.71	0.40: 9	19.71	323.35±41.58	97.48±20.79
h-TiO_2-24.59	0.50: 9	24.59	451.83±86.46	161.72±43.23

Fig. 4-7 shows TEM images of SiO_2@TiO_2 core-shell NPs at TBT: EtOH volume ratio of 0.10: 9 mL (4.95 mM) (Fig. 4-7(a)), 0.2: 9 mL (9.89 mM) (Fig. 4-7(b)) as well as h-TiO_2 at volume ratio of TBT: EtOH were 0.4: 9 mL (19.71 mM) (Fig. 4-7(c)). The results showed that particle size measured by TEM increased from 122.34±10.16 nm to 127.08±4.91 nm with increasing titania precursor. Average particles size from DLS analysis in Table 4-2 shows larger than the particles size from TEM analysis. Shell layer of h-TiO_2 NPs in Fig.4-7(c) was torn and deformed because low condensation rate due to no catalyst in the system, resulting in very thin shell. Aggregation of h-TiO_2 NPs prepared at 19.71 mM was observed, may be resulting in larger average particle size from DLS analysis.

Results from both methods can be summarized as follows; higher temperature performed the complete coating for both methods because of high condensation rate of titanium dioxide. At similar TBT concentration, the particle size prepared from method II has a thinner shell due to lack of catalyst.

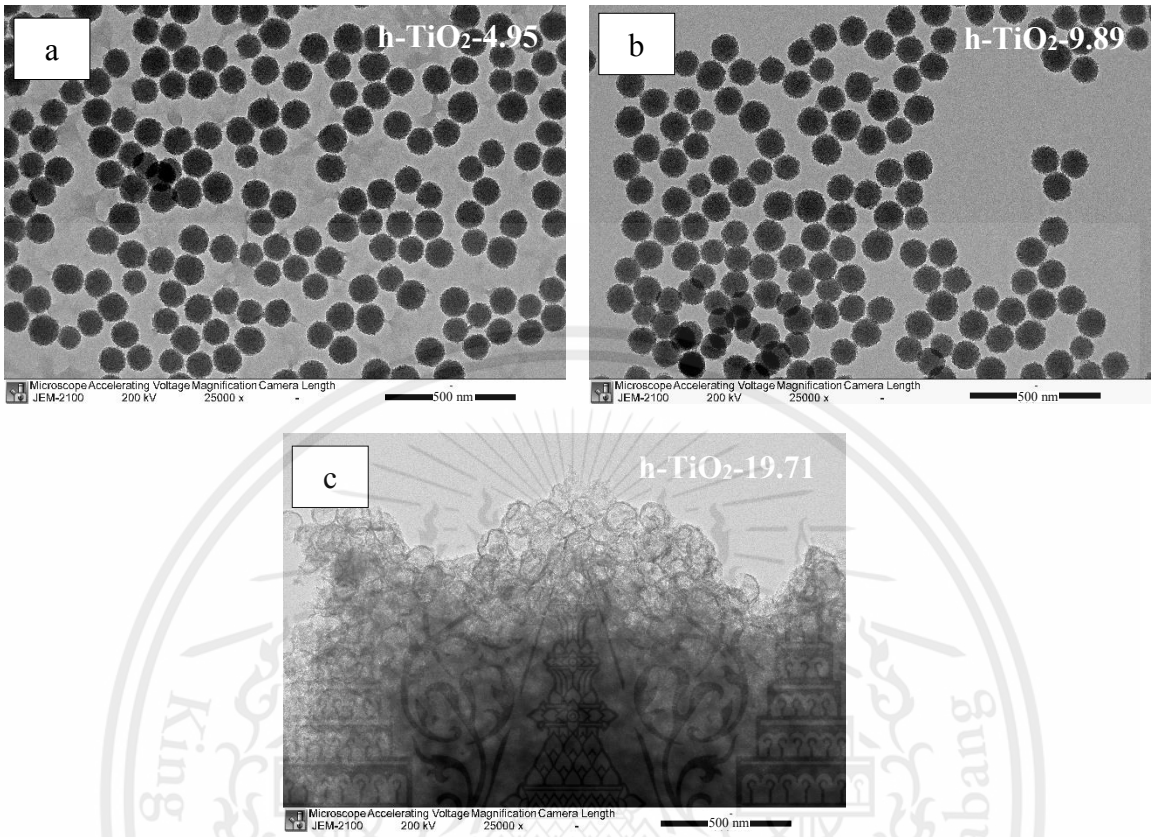

Figure 4-7 TEM images of (a) SiO_2@TiO_2 core-shell NPs at V_{TBT}: V_{EtOH} were 0.1: 9 mL (4.95 mM) (b) SiO_2@TiO_2 core-shell NPs at V_{TBT}: V_{EtOH} were 0.2: 9 mL (9.89 mM) (c) h-TiO_2 at V_{TBT}: V_{EtOH} were 0.4: 9 mL (19.71 mM). These particles were synthesized via method II. Average sizes were measured using ImageJ.

4.3 Optical properties

In this study, shell thickness and particle size were used to indirectly predict optical properties. Razavi-Khosroshahi et al.[43] predict the effect of particle size and shell thickness on the photocatalytic activity of hollow TiO_2 particles. They synthesized hollow TiO_2 NPs at different shell thickness and predict the volume of material that is able to absorb light. Particle with thinner shell thickness has larger of $1/ (R^3_{outer}-R^3_{inner})$ value that show better photocatalytic activity. Therefore, the volume of material should be considered. The volume that can absorb light is related to particle size and shell thickness as equation (1) , where the R_{outer} is the outer radius of the particle and R_{inner} is the inner radius of the hollow particle as showed in Fig. 4-8.

$$V = \frac{3M}{4\pi\rho(R^3_{outer}-R^3_{inner})} \qquad (1)$$

M refers to mass and ρ is density of TiO_2 that is same for all samples. Average particle size and shell thickness were measured using Particle Analyzer, Delsa Nano C of Beckman Coulter.

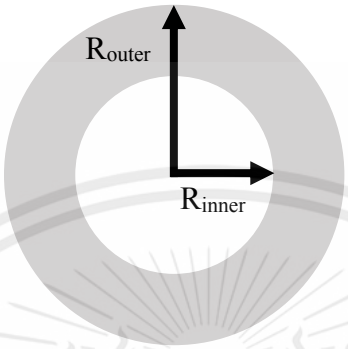

Figure 4-8 Schematic illustration of hollow particle, defining inner radius and outer radius.
Adapted from Razavi-Khosroshahi, H.; Wenhao, S.; Fuji, M. Synthesis of TiO_2 Hollow Nanoparticles with Different Shell Thickness and Effect of Structure on Photocatalytic Activity. Solid State Sci. 2020, 103 (November 2019), 106179. https://doi.org/10.1016/j.solidstatesciences.2020.106179.

Table 4-3 and Table 4-4 shows relation of shell thickness on the absorbing volume of sample prepared from method I and II, respectively. The results showed that particles with thinner shell have a larger of $1/ (R^3_{outer}-R^3_{inner})$ value, indicating better light absorbance but lower light scattering. These results were also consistent with work of Razavi-Khosroshahi et al.[43]. In addition, they support predicted optical properties with UV–vis diffuse reflectance profile of hollow TiO_2 particles with different shell thickness that particles with thinner shell shows more %Absorbance than thick shell.

Table 4-3 Relation of particle size and shell thickness of sample synthesized via method I on V_{absorb}. Size of SiO_2 core was 128.39 nm.

[TBT], mM	Particle size (nm)	Shell thickness (nm)	$1/ (R^3_{outer}-R^3_{inner})$
3.25	170.39±30.89	21.00±15.45	3.5329×10^{-7}
6.49	182.15±86.02	26.88±43.01	2.5464×10^{-7}
8.11	208.78±63.45	40.19±31.73	1.4318×10^{-7}
16.18	227.20±26.35	49.40±13.18	1.0404×10^{-7}

Table 4-4 Relation of particle size and shell thickness of sample synthesized via method II on V_{absorb}. Size of SiO_2 core was 128.39 nm.

[TBT], mM	Particle size (nm)	Shell thickness (nm)	$1/ (R^3_{outer}-R^3_{inner})$
4.95	150.06±20.76	10.84±10.38	7.9197×10^{-7}
9.89	166.05±10.04	18.83±5.02	4.0618×10^{-7}
14.81	274.19±66.18	72.90±33.09	5.4065×10^{-8}
19.71	323.35±41.58	97.48±20.79	3.1553×10^{-8}
24.59	451.83±86.46	161.72±43.23	1.1096×10^{-8}

Hollow TiO_2 NPs synthesized from both methods have predicted results in the same direction. Particles with a thinner shell have lower light scattering. These results point out that morphology, particle size and shell thickness of particles can affect to optical properties. In cosmetic industry, the UV attenuation and size of particles is important for particles act as sunscreen agent. h-TiO_2-3.25 and h-TiO_2-6.49 NPs prepared from method I were suitable for used as sunscreen agent because it has higher light scattering efficiency than the sample prepared with the same TBT concentration and particle size was smaller than 200-nm, resulting in particles do not appear opaque in sunscreen.

Chapter V

Conclusion

h-TiO_2 NPs were successfully synthesized with two different hard template-assisted sol-gel methods. h-TiO_2 NPs prepared from both methods showed that increasing TBT concentration and reaction temperature cause the thicker particle shell due to higher condensation rate. The presence of NH_4OH catalyst, promote the condensation and formation of thicker shell. TEM analysis showed uniform size distribution and homogenous coating. However, aggregation and deformation were found. Particles with thin shell has higher light absorption but lower light scattering. Based on particle size and absorbing volume, h-TiO_2-3.25 and h-TiO_2-6.49 NPs prepared by method I were suitable for used as sunscreen agent.

References

(1) Green, A.; Whiteman, D.; Frost, C.; Battistutta, D. Sun Exposure, Skin Cancers and Related Skin Conditions. *J. Epidemiol.* 1999, *9* (6 Suppl), 7–13. https://doi.org/10.2188/jea.9.6sup_7.

(2) Popov, A. P.; Priezzhev, A. V.; Lademann, J.; Myllyla, R. Alteration of Skin Light-Scattering and Absorption Properties by Application of Sunscreen Nanoparticles : A Monte Carlo Study. *J. Quant. Spectrosc. Radiat. Transf.* 2011, *112*, 1891–1897. https://doi.org/10.1016/j.jqsrt.2011.01.015.

(3) Food and Drug Administration. Ultraviolet (UV) Radiation https://www.fda.gov/radiation-emitting-products/tanning/ultraviolet-uv-radiation#2.

(4) International Agency for Research on Cancer. Chemical and Physical Characteristics of Sunscreen Constituents. In *IARC Handbooks of Cancer Prevention Volume 5*; 2001; pp 17–21.

(5) Zhang, Y.; Qiang, L.; Yuan, Y.; Wu, W.; Sun, B.; Zhu, L. Impacts of Titanium Dioxide Nanoparticles on Transformation of Silver Nanoparticles in Aquatic Environments. *Environ. Sci. Nano* 2018, *00*, 1–3. https://doi.org/10.1039/C8EN00044A.

(6) Labille, J.; Slomberg, D.; Catalano, R.; Robert, S.; Boudenne, J.-L.; Apers-Tremelo, M.-L.; Masion, A.; Garidel, C. DE. Evaluation of the Environmental Exposure to Nanoparticulate UV-Filters Used in Sunscreens. In *Goldschmidt geochemistry conference*; Boston, 2018.

(7) Chen, J.; Saeki, F.; Wiley, B. J.; Cang, H.; Cobb, M. J.; Li, Z.; Au, L.; Zhang, H.; Kimmey, M. B. Gold Nanocages : Bioconjugation and Their Potential Use as Optical Imaging Contrast Agents. *Nano Lett.* 2005, *5*, 1–5. https://doi.org/10.1021/nl047950t.

(8) Thiwakornkitkul, N.; Suteewong, T. Effect of Morphology of Titanium Dioxide Nanoparticles on Photocatalytic Activity. *IOP Conf. Ser. Mater. Sci. Eng.* 2019, *639* (1). https://doi.org/10.1088/1757-899X/639/1/012021.

(9) Wang, Y.; Su, J.; Li, T.; Bai, H.; Xie, Y.; Chen, M.; Dong, W. A Novel UV-Shielding and Transparent Polymer Film : When Bio-Inspired Dopamine-Melanin Hollow Nanoparticles Join Polymer. *ACS Appl. Mater. Interfaces Mater. Interfaces* 2017. https://doi.org/10.1021/acsami.7b08763.

(10) United States Environmental Protection Agency. Sunscreen: The Burning Facts. 2006.

(11) Gasparro, F. P.; Mitchnick, M.; Nash, J. F. A Review of Sunscreen Safety and Efficacy. *Photochem. Photobiol.* 1998, *68* (3), 243–256.

(12) Morabito, K.; Shapley, N. C.; Steeley, K. G.; Tripathi, A. Review of Sunscreen and the Emergence of Non-Conventional Absorbers and Their Applications in

Ultraviolet Protection. *Int. J. Cosmet. Sci.* 2011, *33*, 385–390. https://doi.org/10.1111/j.1468-2494.2011.00654.x.

(13) Tampucci, S.; Burgalassi, S.; Chetoni, P.; Monti, D. Cutaneous Permeation and Penetration of Sunscreens : Formulation Strategies and In Vitro Methods. *Cosmetics* 2018, *5*. https://doi.org/10.3390/cosmetics5010001.

(14) Egerton, T. A.; Tooley, I. R. UV Absorption and Scattering Properties of Inorganic-Based Sunscreens. *Int. J. Cosmet. Sci.* 2012, *34*, 117–122. https://doi.org/10.1111/j.1468-2494.2011.00689.x.

(15) Dutra, E. A.; Almança, D.; Kedor-, E. R. M.; Inês, M.; Miritello, R. Determination of Sun Protection Factor (SPF) of Sunscreens by Ultraviolet Spectrophotometry. 2004, *40* (Equation 1), 381–385.

(16) Lemaster. The ABC's of Ultraviolet Radiation https://www.mcomarin.com/the-abcs-of-ultraviolet-radiation.

(17) Smijs, T. G.; Pavel, S. Titanium Dioxide and Zinc Oxide Nanoparticles in Sunscreens : Focus on Their Safety and Effectiveness. *Nanotechnol. Sci. Appl.* 2011, *4*, 95–112.

(18) Dunford, R.; Salinaro, A.; Cai, L.; Serpone, N.; Horikoshi, S.; Hidaka, H.; Knowland, J. Chemical Oxidation and DNA Damage Catalysed by Inorganic Sunscreen Ingredients. *FEBS Lett.* 1997, *418* (1–2), 87–90. https://doi.org/10.1016/S0014-5793(97)01356-2.

(19) Titanium Dioxide Manufacturers Association. What is titanium dioxide? http://tdma.info/what-is-titanium-dioxide/.

(20) Abrahao, R. T.; Umemura, R.; A, C. B. S. Use of Optical density and TiO_2 light scattering to Identify Optimization Potential In Architectural Coatings. In *European Coatings Congress*; Nürnberg, 2015.

(21) Gupta, R. K.; Bills, B.; Dubey, M.; Galipeau, D.; Fan, Q. H. Light Scattering Behavior of Oxide Nanoparticles. In *IEEE International Conference on Electro-Information Technology*; IEEE: USA, 2013; pp 2–6. https://doi.org/10.1109/EIT.2013.6632673.

(22) Haider, A. J.; Jameel, Z. N.; Al-Hussaini, I. H. M. Review on: Titanium Dioxide Applications. *Energy Procedia* 2019, *157*, 17–29. https://doi.org/10.1016/j.egypro.2018.11.159.

(23) de Dicastillo, C. L.; Patiño, C.; Galotto, M. J.; Vásquez-Martínez, Y.; Torrent, C.; Alburquenque, D.; Pereira, A.; Escrig, J. Novel Hollow Titanium Dioxide Nanospheres with Antimicrobial Activity against Resistant Bacteria. *Beilstein J. Nanotechnol.* 2019, *10*, 1716–1725. https://doi.org/10.3762/bjnano.10.167.

(24) Alexis, A.; Chuberre, B.; Marinovich, M. Safety of Titanium Dioxide Nanoparticles in Cosmetics. *JEADV* 2019, *33*, 34–46. https://doi.org/10.1111/jdv.15943.

(25) Serpone, N.; Dondi, D.; Albini, A. Inorganic and Organic UV Filters : Their Role and Efficacy in Sunscreens and Suncare Products. *Inorganica Chim. Acta* 2007, *360*, 794–802. https://doi.org/10.1016/j.ica.2005.12.057.

(26) Auger, J.; Martinez, V. A.; Stout, B. Theoretical Study of the Scattering Efficiency of Rutile Titanium Dioxide Pigments as a Function of Their Spatial Dispersion. *J. Coat. Technol. Res.* 2009, *6* (1), 89–97. https://doi.org/10.1007/s11998-008-9116-6.

(27) Trivedi, M.; Murase, J. Titanium Dioxide in Sunscreen. In *Application of Titanium Dioxide*; 2017; pp 61–71. https://doi.org/10.5772/intechopen.70121.

(28) Chen, X.; Mao, S. S. Titanium Dioxide Nanomaterials : Synthesis , Properties , Modifications , and Applications. *Chem. Rev.* 2007, *107*, 2891−2959.

(29) Ren, L.; Li, Y.; Hou, J.; Wang, T.; Yang, Y.; Zhao, X. Fabrication and Cavity-Size-Dependent Photocatalytic Property of TiO_2 Hollow Nanoparticles with Tunable Cavity Size. *Mater. Res. Bull.* 2020, *126* (December 2019), 110744. https://doi.org/10.1016/j.materresbull.2019.110744.

(30) El-toni, A. M.; Habila, M. A.; Labis, P. Design, Synthesis and Applications of Core–Shell, Hollow Core, and Nanorattle Multifunctional Nanostructures. *Nanoscale* 2016, *8*, 2510–2531. https://doi.org/10.1039/c5nr07004j.

(31) Mustafa, M. N.; Shafie, S.; Wahid, M. H.; Sulaiman, Y. Light Scattering Effect of Polyvinyl- Alcohol / Titanium Dioxide Nanofibers in the Dye-Sensitized Solar Cell. *Sci. Rep.* 2019, *9*, 1–8. https://doi.org/10.1038/s41598-019-50292-z.

(32) Li, Y.; Yang, D.; Lu, S.; Qiu, X.; Qian, Y.; Li, P. Encapsulating TiO_2 in Lignin-Based Colloidal Spheres for High Sunscreen Performance and Weak Photocatalytic Activity. *ACS Sustain. Chem. Eng.* 2019, *7*, 6234−6242 Research. https://doi.org/10.1021/acssuschemeng.8b06607.

(33) Nakagawa, Y.; Wakuri, S.; Sakamoto, K.; Tanaka, N. The Photogenotoxicity of Titanium Dioxide Particles. *Mutat. Res.* 1997, *394* (April), 125–132.

(34) Huang, N.; Xu, M.; Yuan, C.; Yu, R. The Study of the Photokilling Effect and Mechanism of Ultrafine TiO_2 Particles on U937 Cells I00 I _ ~ Time. *J. Photochem. Photobiol. A Chem.* 1997, *108*, 229–233.

(35) Poljsak, B.; Dahmane, R. Free Radicals and Extrinsic Skin Aging. *Dermatol. Res. Pract.* 2012, *2012*. https://doi.org/10.1155/2012/135206.

(36) Morsella, M.; Alessandro, N.; Lanterna, A. E.; Scaiano, J. C. Improving the Sunscreen Properties of TiO_2 through an Understanding of Its Catalytic Properties. *ACS Omega* 2016, *1*, 464–469. https://doi.org/10.1021/acsomega.6b00177.

(37) Auger, J.; Mcloughlin, D. Theoretical Analysis of Light Scattering Properties of Encapsulated Rutile Titanium Dioxide Pigments in Dependent Light Scattering Regime. *Prog. Org. Coatings* 2014, *77* (11), 1619–1628. https://doi.org/10.1016/j.porgcoat.2014.05.005.

(38) Dadgostar, S.; Tajabadi, F.; Taghavinia, N. Mesoporous Submicrometer TiO_2 Hollow Spheres As Scatterers in Dye-Sensitized Solar Cells. *ACS Appl. Mater. Interfaces* 2012, *4*, 2964–2968. https://doi.org/dx.doi.org/10.1021/am300329p.

(39) Kim, H. J.; Roh, D. K.; Chang, J. H.; Kim, D. SiO_2 Coated Platy TiO_2 Designed for Noble UV / IR-Shielding Materials. *Ceram. Int.* 2019, *45* (May), 16880–16885. https://doi.org/10.1016/j.ceramint.2019.05.231.

(40) Sudjaipraparat, N.; Kaewsaneha, C.; Nuasaen, S.; Tangboriboonrat, P. One-Pot Synthesis of Non-Spherical Hollow Latex Polymeric Particles via Seeded Emulsion Polymerization. *Polymer (Guildf)*. 2017. https://doi.org/10.1016/j.polymer.2017.06.024.

(41) Nuasaen, S.; Tangboriboonrat, P. Optical Properties of Hollow Latex Particles as White Pigment in Paint Film. *Prog. Org. Coatings* 2015, *79* (C), 83–89. https://doi.org/10.1016/j.porgcoat.2014.11.012.

(42) Rama Krishna, C.; Lee, W. M.; Oh, S. Y.; Jeong, K. U.; Yu, Y. T. Improvement in Light Harvesting and Device Performance of Dye Sensitized Solar Cells Using Electrophoretic Deposited Hollow TiO_2 NPs Scattering Layer. *Sol. Energy Mater. Sol. Cells* 2017, *161* (November 2016), 255–262. https://doi.org/10.1016/j.solmat.2016.11.037.

(43) Razavi-Khosroshahi, H.; Wenhao, S.; Fuji, M. Synthesis of TiO_2 Hollow Nanoparticles with Different Shell Thickness and Effect of Structure on Photocatalytic Activity. *Solid State Sci.* 2020, *103* (November 2019), 106179. https://doi.org/10.1016/j.solidstatesciences.2020.106179.

(44) Joo, J. B.; Lee, I.; Dahl, M.; Moon, G. D.; Zaera, F.; Yin, Y. Controllable Synthesis of Mesoporous TiO_2 Hollow Shells: Toward an Efficient Photocatalyst. *Adv. Funct. Mater.* 2013, *23* (34), 4246–4254. https://doi.org/10.1002/adfm.201300255.

(45) Han, C.; Luque, R.; Dionysiou, D. D. Facile Preparation of Controllable Size Monodisperse Anatase Titania Nanoparticles. *Chem. Commun.* 2012, *48* (13), 1860–1862. https://doi.org/10.1039/c1cc16050h.

(46) Ren, G. The Combined Method to Synthesis Silica Nanoparticle by Stöber Process. *J. Sol-Gel Sci. Technol.* 2020, *96*, 108–120. https://doi.org/10.1007/s10971-020-05322-y.

(47) Park, S. K.; Kim, K. Do; Kim, H. T. Preparation of Silica Nanoparticles: Determination of the Optimal Synthesis Conditions for Small and Uniform Particles. *Colloids Surfaces A Physicochem. Eng. Asp.* 2002, *197* (1–3), 7–17. https://doi.org/10.1016/S0927-7757(01)00683-5.

(48) Matsoukas, T.; Gulari, E. Dynamics of Growth of Silica Particles from Ammonia-Catalyzed Hydrolysis of Tetra-Ethyl-Orthosilicate. *J. Colloid Interface Sci.* 1988, *124* (1), 252–261. https://doi.org/10.1016/0021-9797(88)90346-3.

(49) Kim, J. W.; Kim, L. U.; Kim, C. K. Size Control of Silica Nanoparticles and Their

Surface Treatment for Fabrication of Dental Nanocomposites. *Biomacromolecules* 2007, *8* (1), 215–222. https://doi.org/10.1021/bm060560b.

(50) Widoniak, J.; Eiden-Assmann, S.; Maret, G. Synthesis and Characterisation of Porous and Non-Porous Monodisperse TiO_2 and ZrO_2 Particles. *Colloids Surfaces A Physicochem. Eng. Asp.* 2005, *270–271* (1–3), 329–334. https://doi.org/10.1016/j.colsurfa.2005.09.014.

Appendix

Table A-1 Synthesis of SiO_2 nanoparticles: vary volume of precursor (TEOS).

SiO_2 nanoparticles			
Chemical	TEOS	EtOH	NH_4OH
Volume (mL)	3.2, 4.7, 5.7, 7.7	381.5	23.2
Temperature	Room temperature		
Reaction time	9 hours 45 minutes		

Table A-2 Synthesis of SiO_2 nanoparticles: vary volume of catalyst (NH_4OH).

SiO_2 nanoparticles			
Chemical	TEOS	EtOH	NH_4OH
Volume (mL)	3.2, 5.7	381.5	15.5, 23.2
Temperature	Room temperature		
Reaction time	9 hours 45 minutes		

Table A-3 Synthesis of hollow TiO_2 nanoparticles: method I.

Sample	**SiO_2 in EtOH (mL)**	**Ethanol (mL)**	**Acetone (mL)**	**NH_4OH (mL)**	**TBT (mL)**
h-TiO_2-3.25	1.9634	14.5366	28.5	0.15	0.050
h-TiO_2-4.87	1.9634	14.5366	28.5	0.15	0.075
h-TiO_2-6.49	1.9634	14.5366	28.5	0.15	0.100
h-TiO_2-8.11	1.9634	14.5366	28.5	0.15	0.125
h-TiO_2-16.18	1.9634	14.5366	28.5	0.15	0.250
85^{o}C (refluxing condition) and room temperature					
2 hours					

Table A-4 Synthesis of hollow TiO_2 nanoparticles: method II.

Sample	SiO_2 in EtOH (mL)	EtOH (ml)	DI (ml)	TBOT Precursor (ml)	
				TBOT	EtOH
h-TiO_2-4.95	2.3560	47.6440	0.24	0.10	9
h-TiO_2-9.89	2.3560	47.6440	0.24	0.20	9
h-TiO_2-14.80	2.3560	47.6440	0.24	0.30	9
h-TiO_2-19.71	2.3560	47.6440	0.24	0.40	9
h-TiO_2-24.59	2.3560	47.6440	0.24	0.50	9
85°C (refluxing condition)					
100 minutes					

Table A-5 Synthesis of dense TiO_2 nanoparticles.

Sample	MeOH (mL)	$CaCl_2$ (mL)	TTIP (mL)
d-TiO_2-0.03	50	0.2, 0.03 M	0.85
d-TiO_2-0.04	50	0.2, 0.04 M	0.85
Room temperature			
24 hours			

Biography

Name: Nichapat Pukveera

Date of Birth (DD/MM/YY): 10/08/1998

Address: 137/86 Soi Suan Phak 32, Mahasawad, Bangkrui, Nonthaburi, 11130

E-mail: pvr.nichapat@gmail.com

Academic Background:

2017-Present King Mongkut's Institute of Technology Ladkrabang

2011-2016 Satriwatrakhang School

Working Experience: -